The record of the Messinian salinity crisis in the Tertiary Piedmont Basin (NW Italy): the Alba section revisited

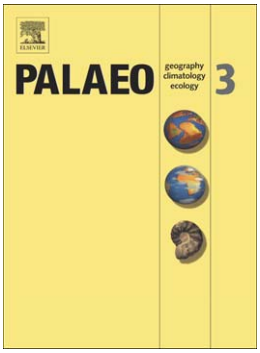

The record of the Messinian salinity crisis in the Tertiary Piedmont Basin (NW Italy): the Alba section revisited

Francesco Dela Pierre, Elisa Bernardi, Simona Cavagna, Pierangelo Clari, Rocco Gennari, Andrea Irace, Francesca Lozar, Stefano Lugli, Vinicio Manzi, Marcello Natalicchio, Marco Roveri, Donata Violanti

PII: S0031-0182(11)00400-7
DOI: doi: 10.1016/j.palaeo.2011.07.017
Reference: PALAEO 5875

To appear in: *Palaeogeography, Palaeoclimatology, Palaeoecology*

Received date: 16 December 2010
Revised date: 7 July 2011
Accepted date: 13 July 2011

Please cite this article as: Dela Pierre, Francesco, Bernardi, Elisa, Cavagna, Simona, Clari, Pierangelo, Gennari, Rocco, Irace, Andrea, Lozar, Francesca, Lugli, Stefano, Manzi, Vinicio, Natalicchio, Marcello, Roveri, Marco, Violanti, Donata, The record of the Messinian salinity crisis in the Tertiary Piedmont Basin (NW Italy): the Alba section revisited, *Palaeogeography, Palaeoclimatology, Palaeoecology* (2011), doi: 10.1016/j.palaeo.2011.07.017

The record of the Messinian salinity crisis in the Tertiary Piedmont Basin (NW Italy): the Alba section revisited

Francesco Dela Pierre[1, 2*], Elisa Bernardi[1], Simona Cavagna[1], Pierangelo Clari[1], Rocco Gennari[3,4], Andrea Irace[2], Francesca Lozar[1], Stefano Lugli[5], Vinicio Manzi[3,4], Marcello Natalicchio[1], Marco Roveri[3,4], Donata Violanti[1,2]

1) Dipartimento di Scienze della Terra, Università di Torino, Via Valperga Caluso 35, 10125, Torino, Italy
2) CNR IGG , Sezione di Torino, Via Valperga Caluso 35, 10125, Torino, Italy
3) Dipartimento di Scienze della Terra, Università di Parma, Via G.P. Usberti 157/A, 43100, Parma (Italy)
4) Alpine Laboratory of Palaeomagnetism (ALP), Via Madonna dei Boschi 76, 12016, Peveragno (CN), Italy

5) Dipartimento di Scienze della Terra, Università degli Studi di Modena e Reggio Emilia, Piazza S. Eufemia 19, 41100, Modena, Italy

* Corresponding author
E-mail adress: francesco.delapierre@unito.it
Phone: +39 0116705198
Fax: +390116705339

ABSTRACT

The Alba succession (Tertiary Piedmont Basin, NW Italy) preserves the northernmost record of the Messinian salinity crisis (MSC) and was deposited on the southern margin of a wide wedge-top basin, related to the involvement of the Piedmont Basin in the Apennine compressional tectonics. Pre-MSC sediments consist of a cyclic succession of marine euxinic shales and calcareous marls, deposited under the influence of precession-modulated climate changes, and document the progressive restriction of the basin prior to the onset of the MSC. They are followed by the Primary Lower Gypsum unit (PLG), deposited during the first MSC stage (from 5.96 to 5.60 Ma). These sediments show a clear precession-related cyclic stacking pattern and record the lateral transition from a shallow water marginal setting in the SW to a deeper one in the NE. In marginal settings, six PLG cycles are recognized, truncated by an erosional unconformity placed at the base of the post-evaporitic sediments. The lowermost five cycles are composed of massive and banded selenite beds separated by thin shale intervals. A sharp change, evidenced by the appearance of the branching selenite facies, is recorded by the 6th gypsum bed that represents a distinctive marker bed, here called Sturani key-bed, that can be mapped throughout the study area. Basinward, the lower PLG cycles are transitional to decimetre-thick dolomite-rich layers interbedded to euxinic shales, that are overlain by the Sturani key-bed. Above the marker bed, other seven PLG cycles are present. The gypsum beds form thinner bodies compared to the Sturani key-bed and are characterized by a greater amount of fine-grained terrigenous fraction, suggesting an increase of continental runoff related, in turn, to humid climate conditions at the end of the first MSC stage. PLG cycles are followed by slumped mudstones and clastic gypsum beds that correspond to the resedimented and chaotic facies (Resedimented Lower Gypsum), deposited in the Mediterranean basins during the second MSC stage (from 5.60 to 5.55 Ma). They are in turn overlain by continental and brackish water facies with Lago Mare fossil assemblages, recording the final stage of the MSC.

The Messinian succession of Alba provides the opportunity to reconstruct the lateral facies transition between marginal and distal settings and to shed new light on the deep water MSC sedimentary record. Moreover, the appearance of the branching selenite facies from the 6th PLG cycle upward provides a tool for properly place the Piedmont record in the MSC

chronostratigraphic framework, allowing to investigate the influence of climate gradients on the sedimentary response to the Mediterranean salinity crisis.

Key words: Messinian salinity crisis, evaporites, Tertiary Piedmont Basin.

1. Introduction

The Messinian salinity crisis (MSC) is one of the major palaeoceanographic event that occurred in the Mediterranean region during the Neogene and was, and still is, the topic of a strong scientific debate. After the discovery of deep-seated Mediterranean evaporites and the formulation of the desiccated deep basin model (Cita, 1973; Hsü et al., 1973; Cita et al., 1978), a wealth of studies has been carried out on the Mediterranean Messinian sediments. The studies have been addressed to both outcropping successions (*e.g.* Butler et al., 1995; Hilgen et al, 1995; Suc et al., 1995; Clauzon et al., 1996; Riding et al., 1998; Krijgsman et al., 1999a, b, 2001; Roveri et al., 2001, 2003; Manzi et al., 2005; Orszag-Sperber, 2006; Roveri et al., 2008a), considered to be mainly deposited in shallow and marginal basins, and to the offshore domain, where seismic profile analyses allowed to image the deep basinal MSC record preserved beneath the abyssal plains of the present-day Mediterranean sea (*e.g.* Ryan, 1976; Lofi et al., 2005; Sage et al., 2005; Maillard et al., 2006; Bertoni and Cartwright, 2007; Lofi et al., 2011). As a matter of fact, different interpretations of the MSC events have been proposed (*e.g.* Rouchy and Caruso, 2006; Ryan, 2009), mainly because a reliable correlation between the onshore and offshore MSC record is not yet available, due to the absence of a continuous drilling of the latter and the lack of its precise stratigraphic calibration. The main controversies regard the amplitude and timing of drawdown phases, the shallow *vs* deep water nature of evaporites, the synchronous *vs* diachronous onset of evaporite deposition, the palaeogeographic status of some Mediterranean sub-basins and the correlation of the shallow and deep water sedimentary record.

Recently a new MSC model, has been proposed, mainly based on the study of the stratigraphic architecture of the Sicilian succession (CIESM, 2008; Roveri, 2008a). The model derives from the two step scenario proposed by Clauzon et al. (1996) and envisages that the MSC developed through three main evolutionary stages. During the first stage (from 5.96 to 5.60 Ma), sulphate evaporites (Primary Lower Gypsum unit; Roveri et al., 2008a) formed in shallow-silled peripheral basins, whereas in deep basinal areas organic-rich shales interbedded to dolomite-rich beds were deposited (Manzi et al., 2007, 2011). The Primary Lower Gypsum (PLG) consists of up to 16 cycles, composed of shales/gypsum couplets. This cyclicity has been ascribed to precession-driven climate changes (Krijgsman et al., 1999a,b; Lugli et al., 2010), thus allowing to date the top of the unit at around 5.60 Ma.

In the second stage (from 5.60 to 5.53 Ma) several lines of evidence suggest a prominent sea level drop. During this stage (MSC acme), the PLG unit underwent subaerial exposure and erosion; the products of erosion were transferred downslope and deposited in deep basins, where they form various types of gravity-driven deposits (chaotic bodies, debris flows, high- to low-density gravity flow deposits). These sediments, firstly described in the Northern Apennines and Sicily (Manzi et al., 2005, 2007; Roveri et al., 2008a) and referred to as Resedimented Lower Gypsum (RLG), locally host thick halite bodies (*e.g.* in the Caltanisetta basin of Sicily). They could correspond to the seismic-defined Lower Unit, recognized offshore in the western Mediterranean basin above pre-MSC sediments (*e.g.* Lofi et al., 2005, 2011). Here, this unit is overlain by thick halite bodies, that has been seismically documented also in the eastern Mediterranean basin (Mobile Unit; Lofi et al., 2011), directly above pre-MSC sediments (Bertoni and Cartwright, 2007).

During the third stage (from 5.53 to 5.33 Ma) a cyclic alternation of gypsum and shales with brackish-water fossil assemblages (Upper Evaporites) was deposited in the SE part of the Mediterranean basin (Sicily, Ionian Islands, Crete, Cyprus and Nile Delta area), whereas shallow to deep water clastic sediments are found in the Apennines and in the Sorbas basin. In the upper part

of these units, fresh and brackish water sediments with Paratethyan fossil assemblages are present, recording the so called Lago Mare event. In the offshore domain, the presence of sediments equivalent to the Upper Evaporites has been suggested in the western Mediterranean basin (*e.g*. Lofi et al., 2011). Conversely, this interval is missing in the eastern Mediterranean basin.

The Messinian section of Alba (Tertiary Piedmont Basin, NW Italy) was one of the reference successions for the interpretation of the complex events of the MSC in the years immediately following the formulation of the deep desiccated basin model (Cita et al., 1978). However, in recent times this succession has been overlooked, despite its study may give important contribution to the understanding of the MSC events at the northern edge of the (palaeo)Mediterranean basin.

The aim of this paper is to provide new data on the stratigraphic architecture of the Messinian succession of the Alba region (Fig. 1), focusing on the PLG unit deposited during the first MSC step, and its lateral equivalents. Field work, consisting of geologic mapping and description, measurement and sampling of six stratigraphic sections (Arnulfi, Rio Berri, Cascina Merlotti, Rocca del Campione, Pollenzo and Santa Vittoria d'Alba, Fig. 2), has been supported by semiquantitative micropaleontologic analyses on foraminifer and calcareous nannofossil assemblages from Arnulfi section, that have been integrated to previous data from the Pollenzo one (Lozar et al., 2009, 2010). Finally, preliminary petrographic studies of carbonate-rich beds and of gypsum lithofacies have been performed. The results of this study have allowed to reconstruct a coherent and updated stratigraphic model of the MSC record of Alba and to correlate it to the recently proposed MSC chronostratigraphic framework (CIESM, 2008).

2. Regional geologic setting

The Tertiary Piedmont Basin (TPB), located on the inner side of SW Alps arc (Fig. 1), is filled with Upper Eocene to Messinian sediments that stratigraphically overlie a complex tectonic wedge of Alpine, Ligurian and Adria basement units juxtaposed in response of the collision between Europe and Adria plates (*e.g.* Roure et al., 1996; Mosca et al., 2009; Rossi et al., 2009) (Fig. 3A). The Cenozoic sediments are presently exposed in the southern (Langhe, Alto Monferrato and Borbera Grue domains) and in the northern (Torino Hill - Monferrato arc) sectors of the TPB (Fig. 1). The relationships between the two outcropping belts are masked by Pliocene to Holocene deposits of the Savigliano and Alessandria basins, but are well imaged by seismic profiles (Bertotti and Mosca, 2009).

Outcrop and seismic data show that the Late Eocene-Oligocene succession consists of continental and shallow marine deposits, accumulated in small fault-bounded basins, followed by deep water Upper Oligocene-Lower Miocene turbidites (Rossi et al., 2009). Since the Late Burdigalian, a more regular physiography was established and the TPB behaved as a single large wedge-top basin, bounded to the north by the uplifted Monferrato arc. The progressive uplift of the southern part of the TPB and its tilting towards the north occurred since the Middle Miocene (Langhian) (Mosca, 2006; Mosca et al., 2009). During the Late Miocene, the north-verging Apennine tectonics involved the Torino Hill area. The N-S crustal shortening was accommodated by further uplift of the southern parts of the TPB and by the establishment of two major subsiding depocentres (Savigliano and Alessandria basins), developed in a piggy-back basin bordered by the Torino Hill - Monferrato tectonic arc (Rossi et al., 2009). This last sector is eventually overthrust to the north onto the Po Plain foredeep, along the Late Neogene to Quaternary Padane thrust front that corresponds to the westward prolongation of the more external Apennine thrusts. The Alba succession, that is the focus of this paper, was deposited on the southern margin of the Savigliano basin, regularly deepening towards the north (Figs. 3A, B).

3. Stratigraphy of the Messinian sediments of the TPB

Messinian sediments are exposed both at the northern and southern margins of the TPB. Most of them, however, are presently buried below the thick cover of Pliocene-Quaternary deposits of the Savigliano and Alessandria basins (Figs. 1, 3A).

The pioneering studies of Sturani (1973, 1976), focused on the Alba region, documented a threefold subdivision of the Messinian succession (Fig. 4). The author recognized a lower pre-evaporitic deep water marine interval (Sant'Agata Fossili Marls, Tortonian-early Messinian), consisting of hemipelagic marls and organic-rich clayey levels (interval 1, Fig. 4) and recording the progressive restriction of the basin prior to the onset of the MSC (Sturani and Sampò, 1973). These sediments are followed by an intermediate evaporitic interval (Gessoso Solfifera Formation), that starts with laminated silty clays and thin stromatolitic limestone beds, considered to be equivalent of the Sicilian "Calcare di Base". This interval (2, Fig. 4) is overlain by laminated euxinic shales (3a, Fig. 4) encasing a 7 m thick laminated microcrystalline primary gypsum bed (known as balatino gypsum) (3b, Fig. 4). Metre-sized masses of selenite, interpreted to be of diagenetic origin, were recognized in the euxinic shales below and above the primary gypsum bed. According to Sturani (1973), these evaporitic sediments were deposited in a hypersaline lagoon: the occurrence of abundant and perfectly preserved continental fossils in the euxinic shales and laminated gypsum, including leaves and delicate dragonfly larvae, indicate that the lagoon was close to a continental area. Episodes of marine incursions, demonstrating the connection with the open ocean, were documented by the occurrence of stenohaline fishes immediately below and above the primary gypsum bed and have been supported by further ichthyologic findings (Cavallo and Gaudant, 1987; Gaudant and Cavallo, 2008) and by the discovery of marine diatom assemblages (Fourtanier et al., 1991; Irace et al., 2005). The upper part of the evaporitic interval consists of laminated silty marls (4a, Fig. 4), deposited under fluctuating salinity conditions, and selenite conglomerates (4b, Fig. 4), up to 2 m thick. According to Sturani (1973), these latter beds "were deposited during flash floods by local torrential streams discharging in the lagoonal environment".

The upper post-evaporitic interval (Cassano Spinola Conglomerates according to Boni and Casnedi, 1970), consists of deltaic to lacustrine terrigenous facies that contain Lago Mare fossil assemblages. These sediments (5, Fig. 4) are in turn overlain by marine Zanclean deposits (Argille Azzurre Fm.) that testify the re-establishment of fully marine conditions after the MSC (Violanti et al., 2009).

The Alba succession has been considered for a long time as the reference section for the Messinian stratigraphy of the TPB. However, field works carried out in the northern and SE sector of the TPB (Dela Pierre et al., 2002, 2007, 2010; Irace et al., 2005) have shown that *in situ* primary evaporites are locally preserved. On the contrary, most of the Messinian gypsum-bearing sediments actually consist of an up to 200 m thick chaotic unit (Valle Versa chaotic complex), that unconformably overlies pre-evaporitic or pre-Messinian sediments. Only locally (Torino Hill, northern edge of the Langhe domain) this unit rests on primary evaporites (Fig. 3B). According to seismic data (Mosca, 2006) the Valle Versa chaotic complex reaches the thickness of 400 m in the Alessandria basin.

The Valle Versa chaotic complex is composed of a fine-grained matrix enveloping blocks of gypsum and of different types of carbonate rocks and is mainly the result of subaqueous mass wasting processes involving the primary shallow water evaporites (Dela Pierre et al., 2002, 2007). Taking into account its characteristics and stratigraphic position, this unit may be considered the equivalent of the RLG unit, deposited in the deep Mediterranean (sub) basins during the second MSC stage (CIESM, 2008). The Valle Versa chaotic complex is unconformably overlain by the Cassano Spinola Conglomerates deposited during the final stages of the MSC, that is after 5.5 Ma.

4. The Alba succession revisited

At Alba, the Messinian succession starts with marine muddy sediments, referred to as the Sant'Agata Fossili Marls, followed by primary evaporites composing the PLG unit. PLG sediments

are followed by slumped and resedimented chaotic gypsum facies and by continental and brackish terrigenous deposits of the Cassano Spinola Conglomerates. These units are described in detail in the following paragraphs.

4.1 The Sant'Agata Fossili Marls

The Sant'Agata Fossili Marls have been studies in the Arnulfi and Pollenzo sections (Figs. 5 and 6), where the transition to the overlying evaporites is also exposed. The unit consists of marine muddy sediments and is characterized by a well defined lithologic cyclicity, given by the alternation of laminated euxinic shale/bioturbated calcareous marl couplets forming up to 3 m thick cycles. These deposits are similar to those described in the coeval euxinic shales of the Vena del Gesso basin (Monte Tondo and Monte del Casino sections; Krijgsman et al., 1997; Vai, 1997; Negri et al., 1999) where the lithologic cyclicity of the pre-MSC deposits has been tuned to the precessional curve.

The fossil content of marly beds consists of foraminifers, calcareous nannofossils, bivalves (*Propeamussium* sp. and *Cuspidaria* sp.), nassarid gastropods, pteropods (*Cavolinia* sp., *Clio* sp, *Limacina* spp.) and land plant debris. The bathyal macroforaminifer *Discospirina* sp. has also been observed. In the euxinic layers, planktonic microfossils and fish remains are present: debris of epi and bathypelagic fishes (*Myctophum* sp., *Alosa elongata*) have been found in the Pollenzo section (Gaudant and Cavallo, 2008; Bonelli, personal communication, 2008).

In the Arnulfi section (SW sector), five shale/marl cycles (Am1-Am5, Fig. 5) are exposed below the first gypsum bed. The upper cycle (Am5) is truncated at the top by a discontinuity surface (see below).

In the Pollenzo section (NE sector) a 80 m thick slumped interval occurs within this unit (Fig. 6). Below the slump seven cycles, showing the above described characteristics, are recognized. Above the slump, the cyclicity is more clearly visible: seven cycles (Pm1-Pm7, Fig. 6) are recognized up to the base of the first gypsum bed (Fig. 7). Each cycle, about 3 m thick, is composed of laminated euxinic shales, transitionally overlain by homogeneous marls that are in turn followed by a 10-15 cm thick carbonate-rich bed and by an upper marl layer (Fig. 8A). The cyclicity is enhanced by regular fluctuations of carbonate content (Fig. 6): in the lower two cycles (Pm1 and Pm2), the carbonate content ranges from 12 % (euxinic shale) to 94 % (carbonate beds). In the upper cycles (Pm3, Pm4, Pm5, Pm6, Pm7) the bulk carbonate content decreases and ranges from 9 % to 47 %. Fossil remains of the euryhaline fish *Aphanius crassicaudus* have been found in the marly layer located immediately below the 6th carbonate-rich bed, within cycle Pm6 (Fig. 6).

All the carbonate-rich beds (*a*-*g*, Fig. 6) show lower and upper transitional contacts and are lithologically similar to the interlayered muds, except for their stronger induration. Bed *a* is the most strongly indurated and contains tubular fossil remains, up to 2 cm long and 0.5 mm across, possibly corresponding to tube worms. Beds *d* and *e* are intensively burrowed and contain centimetre-sized rounded muddy clasts. Beds *f* and *g* are instead strongly laminated: millimetre-thick grey laminae, richer of terrigenous grains, alternate with whitish micritic laminae that are surrounded and crossed by a network of millimetre-wide contractional cracks (Fig. 8B), empty or filled with late diagenetic gypsum crystals and lying both parallel and perpendicular to the bedding. SEM/EDS analyses showed that the most of the authigenic carbonate fraction consists of idiomorphic rombohedral dolomite crystals ranging in size from 2 to 10 μm (beds *a* and *b*, Fig. 8C) or of globular dolomite crystal aggregates commonly developed around a central hollow (Fig. 8D). Pyrite framboids are common, especially in beds *e*, *f* and *g* (Fig. 8E).

4.1.1 Chrono-biostratigraphy

In the lower part of the Pollenzo section (below the slump) and in the Arnulfi one, Messinian planktonic biostratigraphic markers are represented by *Globorotalia conomiozea*, whose First Common Occurrence (FCO), dated at 7.24 Ma (Hilgen et al., 1995), slightly postdates the Tortonian/Messinian boundary, and by *Globorotalia nicolae* whose First Occurrence (FO) (6.83 Ma, Hilgen et al., 1995) was recognized at Pollenzo 10 m above the base of the section (Lozar et al., 2010) (Fig. 6), whereas its Last Occurrence (LO) (6.722 Ma; Hilgen and Krijgsman, 1999; Krijgsman et al., 1999a) has been found at Arnulfi at the base of cycle Am2 (Figs. 5, 6). *Neogloboquadrina acostaensis* left coiled is present in both sections, indicating an age older than 6.337 Ma (*i.e.* the age of s/d coiling change; Sierro et al., 2001; Krijgsman et al., 2004). An abundance peak of *Neogloboquadrina atlantica* (Mediterranean Messinian FCO 6.65 Ma; Blanc-Valleron et al., 2002) occurs in the upper part of the Arnulfi section, documenting an influx of Atlantic cool waters. These data allow correlation of the two sections to the interval Subzone MMi13b (Lourens et al., 2004) (Figs. 5, 6).

The upper cycles of the Sant'Agata Fossili Marls exposed at Pollenzo, above the slump (Fig. 6), are referable to the interval Subzone MMi13c (Lourens et al., 2004) on the basis of the strong impoverishment of foraminifer assemblages, including only rare stress tolerant planktonic (*Turborotalita quinqueloba* and *Turborotalita multiloba*) and benthic (*Bolivina dentellata* and *Bulimina echinata*) taxa. In the lower part *N. acostaensis* right coiled is present, suggesting an age younger than 6.337 Ma The presence of *B. echinata* indicates an age close to or younger than its FO, dated at 6.29 Ma (Kouwenhoven et al., 2006). Planktonic and benthic foraminifers disappear at the top of cycle Pm6, where they are extremely rare and represented by abnormal and dwarf tests of *T. multiloba*, *B. dentellata* and *Brizalina* spp.. The barren upper part of the succession is referable to the Non-distinctive Zone (Iaccarino, 1985; Lourens et al., 2004) (Fig. 6) lasting up to the base of the Pliocene.

In the Arnulfi section the topmost part of the Sant'Agata Fossili Marls is directly overlain by barren silty mudstones, attributed to the Non-distinctive Zone (Lourens et al., 2004) and belonging to the first PLG cycle (Fig. 5). Therefore, a hiatus occurs in this section, encompassing the MMi13c Subzone.

Calcareous nannofossil assemblages are dominated in both sections by long ranging Miocene species (*Reticulofenestra* spp., *Umbilicosphaera* spp., *Discoaster* spp., *Helicosphaera carteri*). The Messinian marker species *Amaurolithus delicatus* is very rare, but is present from the base of the two sections, thus allowing correlation to the MNN11b/c Zone of Raffi et al. (2003).

4.1.2 Palaeoecology

Calcareous plankton

Regular fluctuation of foraminifer and calcareous nannofossil assemblages are documented at Arnulfi and in the lower samples of Pollenzo below the slump. The euxinic shale layers are characterized by abundant warm-water oligotrophic taxa (*e.g. Orbulina* spp. and *Globigerinoides* spp. among foraminifers; *Discoaster* spp. among calcareous nannofossils), whereas the marls contain cool eutrophic taxa, thriving in a well oxygenated water column (i.e *Globigerina bulloides* and Neogloboquadrinids among foraminifers; *Reticulofenestra* spp. and *Umbilicosphaera* spp. among calcareous nannofossil).

At Pollenzo, sediments above the slump yield only rare small planktonics (*T. quinqueloba*), suggesting the establishment of restricted conditions, with the increase of surface water eutrophy (Lozar et al., 2010). Also the calcareous nannofossil assemblages record the same ecological signal, with the sharp abundance peak of *Sphenolithus abies* recorded at the base of cycle Pm5 (Fig. 6); it reflects a palaeoceanographic event slightly preceding the final disruption of the water column at the onset of MSC (see below). The disappearance of the group in cycle Pm7, 3 m below the first gypsum bed (Fig. 6), testifies unfavourable conditions to calcareous nannofossil survival. As mentioned above, these upper pre-evaporitic cycles are not preserved at Arnulfi, due to the hiatus at the top of the Sant'Agata Fossili Marls.

Benthic foraminifers

In the marly beds of the lower part of Pollenzo and Arnulfi sections, benthic foraminifer assemblages are composed of outer neritic to bathyal species (*Cibicidoides pseudoungerianus, Melonis barleanum, Planulina ariminensis* and *Uvigerina* spp.) (Wright, 1978). The upward decrease of specific diversity and the concomitant progressive increase of infaunal buliminids and bolivinids (*B. dentellata*, *Brizalina* spp, *B. echinata*), adapted to low oxygen content and abundant organic matter (Kouwenhoven et al., 2006), suggest the establishment of more restricted conditions, with increasing bottom water disoxia. A shallower and marginal environment is indicated at Arnulfi by the abundance of planktonic foraminifers typical of upwelling areas (*G. bulloides*, *N. acostaensis*) (Hemleben et al., 1989; Sierro et al., 2001) and of benthonic taxa (bolivinids, *Valvulineria bradyana*), adapted to high organic fluxes in shelf setting (Jorissen, 1987). Compared to Pollenzo, bathyal forms (*Cibicidoides kullenbergi*) (van Morkhoven et al., 1986) are rarer in this section. At Pollenzo, above the slump benthic assemblages are poorly diversified and only rare

stress tolerating taxa (*B. dentellata* and *B. echinata*) are present, suggesting bottom waters progressively impoverished in dissolved oxygen and increased stratification of the water column.

4.2 The Primary Lower Gypsum Unit

The Alba PLG unit corresponds, from the lithostratigraphic point of view, to the Vena del Gesso Formation (*sensu* Roveri and Manzi, 2007) and shows a cyclic stacking pattern, evidenced by the rhythmic repetition of laminated silty mudstones and different types of gypsum lithofacies. The most striking feature is a distinct marker bed that can be physically correlated and mapped throughout the study area (Fig. 2), emphasizing a lateral facies change along a SW to NE transect. This marker bed corresponds to the "balatino gypsum bed" of Sturani (1973) (3b, Fig. 4) and thins outward to the NE (Irace et al., 2005). We suggest here to label this marker bed "Sturani key bed" (SKB), thus dedicating it to the memory of the scientist who first provided a comprehensive study of the Messinian successions of the TPB. In the following paragraphs, the stratigraphy of the SW sector, well exposed in the Arnulfi, Cascina Merlotti, Rio Berri and Rocca del Campione sections (Fig. 2) is described separately from that of the NE one, that is exposed in the Pollenzo section.

4.2.1 SW sector

In the Arnulfi section (Figs. 5, 9A) six lithologic cycles (Ag1-Ag6), composed of mudstone/gypsum couplets, are recognized, truncated at the top by the erosional unconformity placed at the base of the post-evaporitic terrigenous sediments (Cassano Spinola Conglomerates). The mudstone layers have an average thickness of 2 m and are strongly laminated, reflecting euxinic bottom conditions. They are very rich in plant debris and locally in dragonfly larvae that appear to be concentrated in silt-sized coarser laminae. Towards the NE in the Rio dei Berri and Cascina Merlotti sections their thickness increases up to 3-4 m.

Gypsum beds composing the three lower cycles (Ag1, Ag2 and Ag3) are only partially exposed and consist of massive selenite. The thickness of these beds is of 10, 5 and 4.5 m respectively. They are made up of decimetre-sized, vertically arranged twinned crystals (Fig. 9B). The size of the crystals is rather constant through the beds. The crystals have a swallow-tail twinning and the angle between the arms of the twin ranges from 30° to 40°. Clayey impurities and elongated peloidal grains are trapped in the re-entrant angle of the twins, giving to the core of the crystals a characteristic cloudy aspect. Very rare "spaghetti like" filaments (*e.g.* Vai and Ricci Lucchi, 1977; Panieri et al., 2010) have been observed.

The fourth and fifth gypsum beds, also recognized in the Rio Berri, Cascina Merlotti and Rocca del Campione sections, are up to 5 m thick and consist of banded selenite (*e.g.* Bąbel, 2007; Lugli et al., 2010). In these beds, roughly tabular layers of vertically oriented twinned crystals having the same size, are separated by thin clayey beds (Fig. 9C). The size of the crystals ranges from 5 to 10 cm and the angle between the arms of the twins is higher than in underlying beds (60°-70°). The larger crystals are concentrated in the lower and upper part of the beds, smaller ones characterize the middle one. Conical structures, up to 2 m across and consisting of clusters of large crystals that grew horizontally or even downward, have been observed at the base of these beds. They are considered as nucleation cones (Lugli et al., 2010), related to the sinking of growing crystals in the underlying muddy substrate.

A sharp facies change is recorded by the 6th bed (SKB), about 10 m thick and characterized by centimetre to metre-sized flat conical structures growing in a laminated matrix, that consists of the regular alternation of millimetre-thick clayey/gypsum laminae (Fig. 10A). The gypsum laminae are composed of tiny (10-20 μm) elongated single crystals or twins that do not show any

preferential orientation but are randomly distributed on the lamina surface (Fig. 10B); this is commonly observed in cumulate deposits made of crystals formed at the water/air surface (or in the water column) and settled down to the bottom. Within clayey-rich laminae, gypsum crystals are less abundant.

The cones are internally formed by millimetre to centimetre-sized selenite crystals with their long axis inclined or oriented horizontally (Fig. 10C). These features have been previously interpreted as early diagenetic products resulting from the displacive growth of coarse-grained selenite masses within the laminated matrix (Sturani, 1973; Clari et al., 2008), because in cross section they show an ellipsoidal shape that gives to the bed a characteristic flaser-nodular structure (embrechitic structure in Sturani, 1973; Vai and Ricci Lucchi, 1977) (Fig. 10D). However, the careful re-examination of these structures has shown that they are identical to the branching selenite facies (Lugli et al., 2010) recently described in the Mediterranean PLG deposits (see below).

In the SW sector, the SKB can be recognized in the Cascina Merlotti and Rocca del Campione sections above the two banded selenite beds. At Rocca del Campione, seven cycles (Rg 4-Rg10, see Fig. 14) are preserved above the SKB, below the erosional unconformity at the base of the Cassano Spinola Conglomerates. These cycles are the same cropping out in the Pollenzo section, that are described in the following paragraph.

4.2.2 NE sector

A different succession is observed in the NE sector (Pollenzo section). Here, below the SKB only two thin (respectively 1.5 and 2 m thick) massive selenite beds (Fig. 11A), consisting of decimetre-sized vertically arranged twinned crystals, are present (Pg1 and Pg2 in Fig. 6). A decimetre-thick discontinuous vuggy carbonate bed is present below the first gypsum layer. The SKB (Figs. 11B, C), shows the same characteristics of the SW sector, but the flat conical structures (branching selenite) are larger (up to 2 m across, Fig. 11D) and are surrounded by a larger amount of laminated matrix.

Above the SKB, seven cycles (Pg4-Pg10, Fig. 6) can be recognized (Fig. 12A), showing the same characteristics than those of Rocca del Campione (cycles Rg4-Rg10, Fig. 14). The gypsum beds composing some cycles (Pg4 and Pg6) are similar to the underlying key bed, except for their reduced thickness (2 and 1.5 m respectively) and the greater amount of clayey fraction (Fig. 12B). In particular the boundary with the underlying mudstones is transitional and is marked by the progressive increase in the amount of gypsum crystals that appear to be dispersed in the terrigenous fraction. In the upper part of these beds, flattened cones, up to 1 m across, have been observed. The other beds (Pg5 and Pg7) are laterally discontinuous and are formed by decimetre-sized cones that float within a matrix of gypsiferous silty mudstones. In the two uppermost beds (Pg9 and Pg10) gypsum crystals, larger than those composing the underlying beds (up to few centimetres long), are dispersed in a muddy matrix and are followed upward by laterally discontinuous flattened cones. These layers have been affected by dissolution of gypsum that is partially replaced by calcite (Fig.

12C). The laminated silty mudstones interbedded to gypsum layers are locally deformed by slumping (*e.g.* cycle Pg8). Remains of *Aphanius crassicaudus*, dragonfly larvae and leaves have been found, commonly within centimetre-thick laminae that are richer in silty terrigenous fraction (commonly represented by mica flakes) than the underlying and overlying ones.

4.3 The post PLG sediments

In the NE sector (Pollenzo), primary evaporites are sharply followed by slumped mudstones, enclosing metre-sized slabs of gypsum similar to those composing the upper PLG cycles (Figs. 13A, B). Carbonate rocks are also involved in the slump. This unit is 5 m thick in the Pollenzo section but becomes thicker toward the NE, *i.e.* towards the distal portion of the basin. In particular, at Santa Vittoria d'Alba (Fig. 2), the slumped sediments are followed by a 5 m thick debris flow that includes metre-sized blocks of selenite floating in a strongly deformed fine-grained matrix. In the northern part of the Alba basin this unit is 20 m thick and is composed of resedimented gypsum beds (gypsrudite and gypsarenite), emplaced by various types of gravity flows and interbedded to euxinic mudstones (Gnavi, 2009).

The upper unit (Cassano Spinola Conglomerates) is composed of continental and brackish water terrigenous deposits (Ghibaudo et al., 1985). At Pollenzo, muddy beds and channelized conglomeratic layers showing large scale cross stratification and containing remains of terrestrial vertebrates (Sardella, 2008) have been observed in the lower part of this unit, together with paleosoil horizons, evidenced by the occurrence of *in situ* root traces. In the upper part, brackish water molluscs *(Congeria, Melanopsis, Limnocardium*) of the Lago Mare biofacies are present, as well as brackish shallow water ostracods (*Amnycithere propinqua*, *Cyprideis agrigentina*, *Loxochonca muelleri*) that allow a correlation with the *Loxoconcha djafarovi* Biozone (Carbonnel, 1978), recognized in the Mediterranean in the post-evaporitic interval (Clari et al., 2008).

5. Discussion: the Alba basin during the Messinian salinity crisis

5.1 Pre-MSC sediments

The cyclic stacking pattern of pre-MSC sediments (Sant'Agata Fossili Marls), evidenced by the rhythmic repetition of marl/euxinic shale couplets and by regular fluctuations of foraminifer and calcareous nannofossil assemblages (Violanti et al., 2007; Lozar et al., 2009; 2010) reflects precession-modulated arid/wet climate changes responsible for deposition of marls at insolation minima and of sapropel or euxinic shales at insolation maxima (*e.g.* Hilgen et al., 1995; Krijgsman et al., 1999a, b; Vazquez et al., 2000; Flores et al., 2005; Kouwenhoven et al., 2006).

Foraminifer and calcareous nannofossil assemblages of the Arnulfi section and of the lower part of the Pollenzo one document a change from open marine to more restricted conditions during the early Messinian, in a time interval encompassing the *G. nicolae* stratigraphic range (6.83-6.72 Ma). A slightly shallower sea bottom is documented by foraminifer assemblages in the SW sector (Arnulfi section), suggesting that deposition of the early Messinian sediments occurred on a northward deepening sea floor (*i.e* the southern margin of the Late Miocene wedge-top basin). According to the biostratigraphic data, a hiatus is present in this section at the top of pre-MSC sediments, possibly related to the sliding of discrete packages of sediments from this marginal sector to the deeper NE area, where they accumulated; this is recorded by the thick slumped interval of the Pollenzo section.

The upper part of pre-MSC sediments is preserved only at Pollenzo above the slump (cycles Pm1-Pm4, Fig. 6), and was deposited in a time interval slightly younger than 6.29 Ma (occurrence of *B. echinata*) up to the onset of the MSC (5.96 Ma), recorded in cycle Pm5, above the peak abundance of *S. abies* (Lozar et al., 2009) (see below). Both foraminifer and calcareous nannofossil

assemblage documents the progressive deterioration of normal marine conditions prior to the onset of MSC, with increasing density stratification, surface salinity and bottom disoxia (Lozar et al., 2010).

5.2 First MSC stage

Primary evaporites composing the PLG unit were deposited at Alba during the first MSC stage (5.96-5.60 Ma, CIESM, 2008). The cyclic stacking pattern, evidenced by the regular alternation of gypsum and mudstone layers, is similar to that described in Mediterranean Lower Evaporites of the marginal basins (*e.g.* Krijgsman et al., 2001; Krijgsman and Meijer, 2008) and is ascribed to precession-related climate changes responsible for deposition of gypsum beds during dry intervals and of laminated mudstones during wet periods. In particular, the mudstone interbeds reflect the dilution of marine brines by undersaturated continental waters (Lugli et al., 2010), responsible for the transport into the basin of variable amounts of terrigenous particles and of terrestrial fossils (leaves, woods, insects) that are locally abundant in these sediments (Sturani, 1973). The concentration of these fossils (especially dragonfly larvae) in silt-sized coarser laminae is consistent with their transport from neighbouring continental areas (Martinetto and Tintori, 2008).

In the SW marginal part of the Alba basin, five cycles occur below the SKB. Due to a relative scarce lateral continuity, these deposits were previously considered of diagnetic origin (gypsum masses in interval 3a, Fig. 4). Actually the gypsum beds composing the lower three cycles (Ag1-Ag3, Fig. 14) consist of massive selenite. This facies suggests deposition in a basin permanently covered by saturated brines; the degree of supersaturation was probably relatively low, allowing the growth of larger crystals (*e.g.* Schreiber and El Tabakh, 2000; Bąbel, 2007; Lugli et al., 2010).

As commonly occurs in other areas of the Mediterranean (Lugli et al., 2010), in the fourth and fifth gypsum beds the dominant facies is represented by banded selenite. The occurrence of superimposed small-sized crystal palisades separated by thin levels of clayey material suggests unstable conditions, dominated by continuous fluctuations of the gypsum saturation surface (*i.e.* the pycnocline, Bąbel 2007) that repeatedly stopped the growth of crystals: as a consequence no large crystals could develop, as in the case of massive selenite (*e.g.* Schreiber, 1978; Lu, 2006; Bąbel, 2007). According to Lugli et al. (2010) these conditions suggest a minimum level of the saturated brines: in particular, the banded selenite facies would mark the peak of aridity in the cyclical deposition of evaporites.

The vertical transition from massive to banded selenite indicates an increase of brine concentration during the early stages of the MSC, due to continuous evaporation and drawdown (Roveri et al., 2008b; Lugli et al., 2010). The real depth of formation of these facies is debated, since no modern analogues exist: however the occurrence of cyanobacteria filaments, often included in the core of the crystals in many Mediterranean examples (*e.g.* Vai and Ricci Lucchi, 1977; Panieri et al., 2010) has suggested relatively shallow depth, within the photic zone, although the depth of growth of such bacterial mats is not clear (Lugli et al., 2010). These features are rare in the studied outcrops, possibly suggesting slightly deeper depositional conditions or a turbid water column, due to abundant suspended clayey particles, not suitable for the penetration of light. The same gypsum facies described in the Mediterranean have been interpreted as deposited at depth lower than 100 - 200 m (Lugli et al., 2010).

The two massive selenite beds that occur in the Pollenzo section below the SKB (Pg1 and Pg2) can be correlated to the banded selenite layers that, in the SW compose the fourth and fifth cycles (Ag4 and Ag5). Consequently the lower three mudstone/massive selenite cycles found at the basin margin (Ag1, Ag2 and Ag3) should correspond, in a more distal position, to the uppermost cycles (Pm5, Pm6 and Pm7) at the top of the Sant'Agata Fossili Marls (Fig. 14), that are composed of shales and dolomite-rich carbonate beds. Hence these evaporite-free cycles can be regarded as

the deeper water counterpart of the lower PLG cycles deposited in the marginal part of the basin (Fig.15). This hypothesis is confirmed by biomagnetostratigraphic analyses performed on the upper part of the Pollenzo section (Lozar et al., 2009, 2010) that have shown that the onset of MSC should be placed at the base of cycle Pm5, few metres above the peak abundance of the calcareous nannofossil *S. abies*. This event can be correlated with other sections in the Mediterranean region (Wade and Bown, 2006; Manzi et al., 2007), where it approximates the onset of the MSC.

Barren shales and dolomite-rich levels have been reported in different Mediterranean areas (*e.g.* Manzi et al., 2007; de Lange and Krijgsman, 2010; Manzi et al., 2011). Their deposition was driven by the occurrence of anoxic bottom conditions related to a density stratified water column (*e.g.* Bąbel, 2007; de Lange and Krijgsman, 2010). Petrographic features of the Alba dolomite-rich beds (globular aggregates and empty spheroidal dolomite crystals) strongly suggest that dolomite precipitation was triggered by microbial activity, at a geochemical interface parallel to the sea floor (*e.g.* Oliveri et al., 2010). At this regard, observations on present-day settings and culture experiments (Vasconcelos et al., 1995; Meister et al., 2008) have shown that dolomite precipitation in anaerobic, organic carbon-rich sediments, can be driven by sulphate reducing bacteria that, by degrading organic matter, consume sulphate ions and increase alkalinity of pore waters, thus overcoming kinetic inhibition to dolomite precipitation (Wright and Oren, 2005). At the same time the decrease of sulphate concentration can slow or hinder gypsum deposition (Bąbel, 2007; Krijgsman and Meijer, 2008). Sulphate reduction produces sulphides, that can further precipitate as Fe sulphides if iron is available from pore waters. Even if further geochemical data are needed to confirm the role of bacteria in dolomite precipitation, the common occurrence of pyrite framboids in the Pollenzo dolomite-rich layers supports this hypothesis.

Gypsum deposition could start in this deeper setting only when the drop of brine level, driven by continuous evaporative drawdown, caused the shift of the oxygen-depleted zone basinward, thus inhibiting sulphate reducing bacteria activity and allowing the bottom growth of large selenite crystals (massive selenite) on the now oxygenated sea bottom. These beds correspond, in the marginal sector, to the banded selenite facies (Fig. 15) that formed during interval of minimum brine level and increased brine concentration.

A prominent change in facies association is recorded from the 6th PLG cycle (SKB) upward (Figs. 14, 15). This change is evidenced by the disappearance of the massive and banded selenite and by the appearance of the branching selenite facies; moreover, it is accompanied by the homogenisation of the depositional conditions, with the ubiquitous deposition of the upper PLG cycles both in marginal and distal setting. The branching selenite facies was originally described in the Vena del Gesso basin as nodular and lenticular selenite (Vai and Ricci Lucchi, 1977) and was considered as rehydrated secondary gypsum, resulting from previous anhydrite nodules formed in a sabhka environment. Recently, Lugli et al. (2010) have re-interpreted this gypsum facies as primary; according to this new hypothesis these deposits consist of bottom grown small-sized selenite crystals grouped in branches projecting outward from a common nucleation cone. Moreover, the branching selenite is considered as an evolution of the supercone structures described by Dronkert (1985) in the Sorbas Basin but with a less evident conical shape. Its development would be strongly related to a current dominated brine flow, able to inhibit the vertical growth of the crystals and to force their lateral development. At Alba the deposition of branching selenite was accompanied by gypsum cumulate deposition, *i.e.* crystals formed at the air/water interface and settled to the bottom, punctuated by shale deposition during wet episodes.

Lugli et al. (2010) have suggested that the branching selenite facies appears from the 6th PLG cycle (*i.e.* at around 5.84 Ma) at the Mediterranean scale, providing a tool for bed by bed correlations among sections located thousands of km apart. Its synchronous appearance would suggest a basin-wide hydrologic change, concomitant with an increased input of Atlantic water in the Mediterranean as suggested by the shift of Sr isotope contrasting with the stronger continental signature of the lower cycles (Lugli et al., 2007). Although no Sr isotope data are yet available for the TBP, such an increase of the oceanic water input in the Mediterranean during the same time

period is supported by the occurrence of stenohaline fishes and of marine diatom assemblages in the euxinic mudstones immediately below and above the SKB (*i.e* from the 6th cycle upward) (Sturani, 1973; Cavallo and Gaudant, 1987; Fourtanier et al., 1991; Gaudant and Cavallo, 2008). These paleontologic findings forced Sturani (1973) to stress the connection of the Alba basin with the open ocean, in strong contrast with the theory of the dessication of the Mediterranean basin that was predominant at that time.

The influx into the basin of marine waters was superimposed to a general shallowing upward trend, suggested by the ubiquitous deposition of the SKB and of the upper cycles in both marginal (Rocca del Campione section) and distal settings (Pollenzo section). These upper PLG cycles are characterized by higher clayey terrigenous input that became predominant, with only minor scattered gypsum deposits; this points to an effective continental runoff from the neighbouring emerged Alpine chain and suggests the influence of humid climate conditions at the end of the first MSC step. The increased clayey input in the basin may have played a role in the disappearance of large swallow-tail crystals, since rapidly buried nuclei could not develop large upward growing crystals.

5.3 Second and third MSC stage

Slumped and chaotic sediments, grading towards the north (*i.e.* towards the distal part of the basin) to clastic evaporites emplaced by various types of gravity flows (Gnavi, 2009) were deposited during the second MSC stage (5.60-5.55 Ma; CIESM, 2008) (Fig. 15). These sediments correspond to interval 4b of Sturani (1973) (Fig. 14) and to the chaotic unit (Valle Versa chaotic complex) recognized in the northern and eastern sectors of the TPB and in the Savigliano and Alessandria depocentres (Mosca et al., 2009) and are considered as equivalent to the Resedimented Lower Gypsum unit deposited in some basinal Mediterranean areas (*e.g.* Manzi et al., 2005). In the TPB, the basal surface of these chaotic sediments is sharp erosional, and locally cuts the underlying sediments down to the Tortonian (Irace et al., 2005). This surface is correlated to the Messinian Erosional Surface (Dela Pierre et al., 2007), recognized at the Mediterranean margins and commonly related to an evaporative sea level-drop of at least 1500 m during the MSC acme, leading to subaerial exposure and erosion of marginal Mediterranean areas *(e.g.* Lofi et al., 2011). However, in the TPB this surface is associated to an angular unconformity, clearly recognized in the northern margin of the basin (Monferrato and Torino Hill area) and generated by the overthrusting of the TPB onto the Po Plain foredeep along the north-verging Padane thrust front (Dela Pierre et al., 2007). This suggests that intra-Messinian tectonic activity played the major role in triggering subaqueous large scale mass wasting phenomena, responsible for the widespread erosion of the basin margins and for the emplacement of chaotic deposits. At Pollenzo, thirteen PLG cycles are preserved below the Messinian Erosional Surface, suggesting that 3-4 cycles are missing (Fig. 15).

The chaotic sediments are finally followed by continental and brackish water Lago-Mare facies (Cassano Spinola Conglomerates) deposited during the final stages of the MSC (5.5-5.33 Ma; CIESM, 2008). The basal surface of these sediments is an erosional surface cutting locally the underlying succession down to the SKB (Figs. 14, 15) and probably reflecting the further tectonic uplift of the basin margins, due to ongoing north-verging Apennine compressional tectonics.

6. Concluding remarks

One of the most controversial points of the MSC regards the correlation between marginal basins (that provide most of the outcropping successions) and deep basinal areas, whose sedimentary record is still poorly known, mainly because it is buried below the abyssal plains of the Mediterranean sea (*e.g.* CIESM, 2008). Outcrop-based studies aimed to the reconstruction of the sedimentary record of area connecting marginal and basinal zones may contribute to solve the controversy. Unfortunately, transitional zones are rarely preserved in the geologic record, mainly

because they corresponded to structurally-controlled slopes that were subjected to later post depositional destabilization.

The Alba succession was deposited on the southern margin of a large wedge-top basin, characterized by a wide and deep depocentral zone (now buried under the Pliocene-Quaternary sediments of the Savigliano basin) and bounded by a northern uplifted sill corresponding to the Torino Hill-Monferrato arc. This peculiar situation provides an opportunity for the reconstruction of the stratigraphic and genetic relationship among facies deposited on a transition zone connecting a shallow marginal area to a deeper basinal sector. The collected data indicate that massive selenite beds pass basinward to euxinic mudstones interbedded with dolomite-rich layers deposited on an anoxic sea bottom, in agreement to what recently proposed (Manzi et al., 2007; Lugli et al., 2010; Manzi et al., 2011). However, dolomitic beds comparable to those forming the deep water counterparts of gypsum are also present in the upper part of the pre-evaporitic succession, from around 6.04 Ma (Fig. 15). The onset of gypsum deposition is diachronous over a lateral distance of few km and is progressively younger basinward. In the Pollenzo section, the deposition of the first massive selenite bed is delayed of three precessional cycles with respect to the marginal part of the basin, where the time equivalent facies consists of banded selenite (Fig. 15).

The appearance of the branching selenite facies from the 6th PLG cycle onward provides a tool for the correlation of the TPB succession. *i.e* the northernmost record of the Mediterranean salinity crisis, to the MSC chronostratigraphic framework, allowing to investigate the influence of climate gradients on the sedimentary response of the MSC and on the hydrologic changes that occurred at the NW termination of the Adriatic gulf, at the foot of the Western Alps. Overall evidence indicate that humid climate conditions, responsible for the increase of continental runoff from the neighbouring Alpine chain and of the input of clay in the basin, developed from around 5.84 Ma, together with episodes of marine incursion. This is consistent with available micro- (pollen) and macro- (leaves, fruit and seeds) paleobotanical data, that strongly suggest that the western prolongation of the Adriatic-Padane basin would have been under predominant moist conditions during the first MSC step and that severe climate gradients affected the Mediterranean basin during this interval (Bertini and Martinetto, 2011). At this regard, it should be stressed that the TPB paleobotanical data set comes from sections where only the upper PLG cycles are exposed.

The second stage of the MSC is recorded by slumped and chaotic facies equivalent of the Resedimented Lower Gypsum unit. In the deeper part of the Alba basin (*i.e.* Pollenzo section) these sediments directly overlies, through the Messinian erosional surface, the PLG unit (Fig. 15), unlike other Mediterranean examples where the resedimented facies are developed above their deep water counterpart, *i.e.* barren euxinic shales. Finally, continental and brackish water sediments with Lago Mare fossil assemblages were deposited during the third MSC stage, above an erosional unconformity that sharply cuts the underlying succession.

Further research is needed on the TPB succession, especially devoted to the reconstruction of the palaeonvironmental and palaeohydrologic change heralding the onset of the MSC, to the characterization of the deep water counterpart of the evaporites, and to the definition of the stratigraphic architecture of the Lago Mare sediments, still poorly known. At this regards, the Pollenzo section stands as a key section for the reconstruction of the MSC events at the northern edge of the Mediterranean basin, in a transition zone connecting a shallow marginal area with a deep basinal sector.

Acknowledgements

The authors would like to thank E. Bonelli, O. Cavallo and E. Martinetto for assistance in the field and paleontologic informations. P. Mosca and M. Rossi are thanked for their suggestions and discussions. Advice and criticisms of F. Surlyk and of two anonymous reviewers greatly improved the manuscript. Research funded by MIUR grants to D. Violanti (PRIN-COFIN 2008).

References

Bąbel, M., 2007. Depositional environments of a salina type evaporite basin recorded in the Badenian gypsum facies in northern Carpathian Foredeep, In: Schreiber, B. C., Lugli, S., Bąbel, M. (Eds), Evaporites Through Space and Time. Geological Society of London, Special Publication 285, pp.107-142.

Bertini, A., Martinetto, E., 2011. Reconstruction of vegetation transects for the Messinian-Piacenzian of Italy by means of comparative analysis of pollen, leaf and carpological records. Palaeogeography, Palaeoclimatology, Palaeoecology, 304, 230-246.

Bertoni, C., Cartwright, A., 2007. Major erosion at the end of the Messinian salinity crisis: evidence from the Levant basin, eastern Mediterranean. Basin Research, 19, 1365-2117.

Bertotti, G., Mosca, P., 2009. Late orogenic vertical movements within the arc of the SW Alps and Ligurian Alps. Tectonophysics 475, 117-127.

Bigi, G., Cosentino, D., Parotto, M., Sartori, R., Scandone, P., 1990. Structural Model of Italy: Geodinamic Project: Consiglio Nazionale delle Ricerche, S.EL.CA, scale 1:500,000, sheet 1.

Blanc-Valleron, M.M., Pierre, C., Caulet, J.P., Caruso, A., Rouchy, J.M., Cespuglio, G., Sprovieri, R., Pestrea, S., Di Stefano, E., 2002. Sedimentary, stable isotope and micropaleontological records of paleoceanographic change in the Messinian Tripoli Formation (Sicily, Italy). Palaeogeography, Palaeoclimatology, Palaeoecology 185, 255-286.

Boni, A., Casnedi, R., 1970. Note illustrative della Carta Geologica d'Italia alla scala 1:100.000, Fogli 69-70, Asti e Alessandria. Poligrafica e Carte Valori, Ercolano (Na), pp. 64.

Butler, R.W.H., Lickorish, W.H., Grasso, M., Pedley, H.M., Ramberti, L., 1995. Tectonics and sequence stratigraphy in Messinian basins, Sicily: constraints on the initiation and termination of the Mediterranean salinity crisis. Geological Society of America Bulletin 107, 425-439.

Carbonnel, G., 1978. La zone a *Loxoconcha djaffarovi* Schneider (Ostracoda, Miocène supérieur) ou le Messinien de la Vallée du Rhône. Revue de Micropaléontologie 21, 106-118.

Cavallo, O., Gaudant, J., 1987. Observations complémentaires sur l'ichthyofaune des marnes Messiniennes de Cherasco (Piémont): implications géodynamiques. Bollettino della Società Paleontologica Italiana 26, 177-198.

CIESM, 2008. The Messinian Salinity Crisis from mega-deposits to microbiology – A consensus report. CIESM Workshop Monographs N° 33, F. Briand Eds, Monaco, pp.168.

Cita, M.B., 1973. Mediterranean evaporite: paleontological arguments for a deep basin desiccation model, In: Messinian Events in the Mediterranean. Kon. Ned. Akad. Wetensch, Amsterdam, 203-223.

Cita, M.B., Wright, R.C., Ryan, W.B.F., Longinelli, A., 1978. Messinian paleoenvironments, In: Hsü, K.J., Montadert, L. et al. (Eds.), Initial Reports of the Deep Sea Drilling Project 42. U.S. Government Printing Office, Washington D.C, 1003-1035.

Clari, P, Bernardi, E., Cavagna, S., Dela Pierre, F., Irace, A., Lozar, F., Martinetto, E., Trenkwalder, S., Violanti, D., 2008. Guida all'Escursione. Convegno Alba e Tramonto della crisi Messiniana, Alba 10-11 ottobre 2008. Dipartimento di Scienze della Terra Università di Torino, pp. 43.

Clauzon, G., Suc, J.P., Gautier, F., Berger, A., Loutre, M.F., 1996. Alternative interpretation of the Messinian salinity crisis: controversy resolved? Geology 24, 363-366.

de Lange, G. J., Krijgsman, W., 2010. Messinian salinity crisis: a novel unifying shallow gypsum/deep dolomite formation mechanism. Marine Geology 275, 273-277.

Dela Pierre, F., Clari, P., Cavagna, S., Bicchi, E., 2002. The Parona chaotic complex: a puzzling record of the Messinian (Late Miocene) events in Monferrato (NW Italy). Sedimentary Geology 152, 289-311.

Dela Pierre, F., Festa, A., Irace, A., 2007. Interaction of tectonic, sedimentary and diapiric processes in the origin of chaotic sediments: an example from the Messinian of Torino Hill (Tertiary Piedmont Basin, northwestern Italy). Geological Society of America Bulletin 119, 1107-1119.

Dela Pierre, F., Martire, L., Natalicchio, M., Clari, P.A., Petrea, C., 2010. Authigenic carbonates in the upper Miocene sediments of the Tertiary Piedmont Basin (NW Italy): vestiges of an ancient gas hydrate stability zone? Geological Society of America Bulletin 122, 994-1010.

Dronkert, H., 1985. Evaporite models and sedimentology of Messinian and recent evaporites. GUA Papers Geology, (Amsterdam), Serials I 24, pp. 283.

Flores, J.A., Sierro, F.J., Filippelli, G.M., Barcena, M.A., Perez-Folgado, M., Vazquez, A., Utrilla, R., 2005. Surface water dynamics and phytoplankton communities during deposition of cyclic late Messinian sapropel sequences in the western Mediterranean. Marine Micropaleontology 56, 50-79.

Fourtanier, E., Gaudant, J., Cavallo, O., 1991. La diatomite de Castagnito (Piémont): une nouvelle preuve de l'existence d'oscillations modérées du niveau marine pendant le Messinien évaporitique. Bollettino della Società Paleontologica Italiana 30, 79-95.

Gaudant, J., Cavallo, O., 2008. The Tortonian-Messinian fish faunas of Piedmont (Italy) and the Adriatic trough: a synthesis dedicated to the memory of Carlo Sturani (1938-1975). Bollettino della Società Paleontologica Italiana 47, 177-189.

Ghibaudo, G., Clari, P., Perello, M., 1985. Litostratigrafia, sedimentologia ed evoluzione tettonico-sedimentaria dei depositi miocenici del margine sud-orientale del Bacino Terziario ligure-piemontese (Valli Borbera, Scrivia e Lemme). Bollettino della Società Geologica Italiana 104, 349-397.

Gnavi, L., 2009. La successione messiniana del Bacino Terziario Piemontese: dati stratigrafici di affioramento e di sottosuolo, caratterizzazione geochimica e palinologica. Unpublished graduation thesis, University of Turin, pp. 214.

Hemleben, C., Spindler, M., Anderson, O.R., 1989. Modern Planktonic Foraminifera. Springer-Verlag, Berlin.

Hilgen, F.J., Krijgsman, W., Langereis, C.G., Lourens, L.J., Santarelli, A., Zachariasse, W.J., 1995. Extending the astronomical (polarity) time scale into the Miocene. Earth and Planetary Sciences Letters 136, 495-510.

Hilgen, F.J., Krijgsman, W., 1999. Cyclostratigraphy and astrochronology of the Tripoli diatomite Formation (pre-evaporite Messinian, Sicily, Italy). Terra Nova 11, 16-22.

Hsü, K.J., Cita, M.B., Ryan, W.B.F., 1973. The origin of the Mediterranean evaporites, In: Ryan, W.B.F., Hsü, K.J., et al. (Eds.), Initial Report of Deep Sea Drilling Program 13. U.S. Government Printing Office, Washington DC, pp. 1203-1231

Kouwenhoven, T. J., Morigi, C., Negri, A., Giunta, S., Krijgsman, W., Rouchy, J. M., 2006. Palaeoenvironmental evolution of the eastern Mediterranean during the Messinian: constraints from integrated microfossil data of the Pissouri Basin (Cyprus). Marine Micropalaeontology 60, 17-44.

Krijgsman, W., Hilgen, F.J., Negri, A., Wijbrans, J.R., Zachariasse, W.J., 1997. The Monte del Casino section (Northern Apennines, Italy): a potential Tortonian/Messinian boundary stratotype? Palaeogeography, Palaeoclimatology, Palaeoecology 133, 27-48.

Krijgsman, W., Hilgen, F.J., Marabini, S., Vai, G.B., 1999a. New paleomagnetic and cyclostratigraphic age constraints on the Messinian of the Northern Apennines (Vena del Gesso Basin, Italy). Memorie della Società Geologica Italiana 54, 25-33.

Krijgsman, W., Hilgen, F.J., Raffi, I., Sierro, F.J., Wilson, D.S., 1999b. Chronology, causes and progression of the Messinian salinity crisis. Nature 400, 652-655.

Krijgsman, W., Fortuin, A.R., Hilgen, F.J., Roep, T.B., Sierro, F. J., 2001. Astrochronology for the Messinian Sorbas Basin (SE Spain) and orbital (precessional) forcing for evaporite cyclicity. Sedimentary Geology 140, 43-60.

Krijgsman, W., Gaboardi, S., Hilgen, F.J., Iaccarino, S., de Kaenel, E., van der Laan, E., 2004. Revised astrochronology for the Ain el Beida section (Atlantic Morocco): no glacio–eustatic control for the onset of the Messinian Salinity Crisis. Stratigraphy 1, 87-101.

Krijgsman, W., Meijer P.T., 2008. Depositional environments of the Mediterranean "Lower Evaporites" of the Messinian salinity crisis: constraints from quantitative analyses. Marine Geology 253, 73-81.

Iaccarino, S., 1985. Mediterranean Miocene and Pliocene planktic Foraminifera, In: Bolli, H. M., Saunders, J. B., Perch-Nielsen, K., (Eds.), Plankton Stratigraphy. Cambridge University Press, Cambridge, pp. 283-314.

Irace, A., Dela Pierre, F., Clari P., 2005. "Normal" and "chaotic" deposits in the Messinian Gessoso-Solfifera Fm. at the North-Eastern border of the Langhe domain (Tertiary Piedmont Basin). Bollettino della Società Geologica Italiana, Special Publication 4, 77-85.

Jorissen, F. J., 1987. The distribution of benthic foraminifera in the Adriatic Sea. Marine Micropaleontology 12, 21-48.

Lofi, J., Gorini, C., Berne, S., Clauzon, G., Dos Reis, A.T., Ryan, W.B.F. and Steckler, M. S., 2005. Erosional processes and paleo-environmental changes in the western gulf of Lions (SW France) during the Messinian Salinity Crisis. Marine Geology 217, 1-30.

Lofi, J., Sage, F., Déverchère, J., Loncke, L., Maillard, A., Gallier, V., Thinon, I., Gillet, H., Guennoc, P., Gorini, C., 2011. Refining our knoweldge of the Messinian salinity crisis in the offshore domain through multi-site seismic analysis. Bulletin Société Géologique de France, 182, 163-180.

Lourens, L., Hilgen, F., Shackleton, N.J., Laskar, J., Wilson, D., 2004. The Neogene period, In: Gradstein, F.M., Ogg, J.G., Smith, A.G., (Eds.), A geologic time scale 2004. Cambridge University Press, pp. 409-440.

Lozar, F., Bernardi, E., Violanti, D., Dela Pierre, F., Gennari, R., Clari, P. Cavagna, S., Irace, A., Lanza, R., 2009. Biomagnetostratigraphic data on the Pollenzo section: new insight on the onset of the Messinian Salinity Crisis, 13th Congress RCMNS, 2-6 september 2009, Naples, Italy. Acta Naturalia de l'Ateneo Parmense 45, 376-378.

Lozar, F., Violanti, D., Dela Pierre, F., Bernardi, E., Cavagna, S., Clari P., Irace, A., Martinetto, E., Trenkwalder, S., 2010. Calcareous nannofossils and foraminifers herald the Messinian salinity crisis: the Pollenzo section (Alba, Cuneo; NW Italy). Geobios 43, 21-32.

Lu, F.H., 2006. Lithofacies and water-body record of Messinian evaporites in Nijar Basin, SE Spain. Sedimentary Geology 188–189, 115-130.

Lugli, S., Bassetti, M.A., Manzi, V., Barbieri, M., Longinelli, A., Roveri, M., 2007. The Messinian 'Vena del Gesso' evaporites revisited: characterization of isotopic composition and organic matter, In: Schreiber, B.C., Lugli, S., Bąbel, M., (Eds), Evaporites Through Space and Time. Geological Society of London, Special Publication 285, 143-154.

Lugli, S., Manzi, V., Roveri, M., Schreiber, B.C., 2010. The Primary Lower Gypsum in the Mediterranean: a new facies interpretation for the first stage of the Messinian salinity crisis. Palaeogeography, Palaeoclimatology, Palaeoecology 297, 83-99.

Maillard, A., Gorini, C., Mauffret, A., Sage, F., Lofi, J., Gaullier, V., 2006. Offshore evidence of polyphase erosion in the Valencia basin (northwestern Mediterranean): scenario for the Messinian salinity crisis. Sedimentary Geology 188-189, 69-91.

Manzi, V., Lugli, S., Ricci Lucchi, F., Roveri, M., 2005. Deep-water clastic evaporites deposition in the Messinian Adriatic foredeep (northern Apennines, Italy): did the Mediterranean ever dry out? Sedimentology 52, 875-902.

Manzi, V., Roveri, M., Gennari, R., Bertini, A., Biffi, U., Giunta, S., Iaccarino, S., Lanci, L., Lugli, S., Negri, A., Riva, A., Rossi, M.E., Taviani, M., 2007. The deep-water counterpart of the Messinian Lower Evaporites in the Apennine foredeep: the Fanantello section (Northern Apennines, Italy). Palaeogeography, Palaeoclimatology, Palaeoecology 251, 470-499.

Manzi, V., Lugli, S., Roveri, M., Schreiber, B.C., Gennari, R., 2011. The Messinian "Calcare di Base" (Sicily, Italy) revisited. Geological Society of America Bulletin 123, 347-370.

Martinetto, E., Tintori, A., 2008. Tafonomia e indicazioni paleoambientali delle associazioni a pesci, piante e insetti dei sedimenti messiniani di Alba. In, Alba e tramonto della crisi Messiniana. Alba 10-11 ottobre 2008, Abstract, pp. 47-48.

Meister, P., Bernasconi, S.M, Vasconcelos, C., McKenzie, J.A., 2008. Sea level changes control diagenetic dolomite formation in hemipelagic sediments of the Peru Margin. Marine Geology 252, 166-173.

Mosca, P., 2006. Neogene basin evolution in the Western Po Plain, NW Italy: insights from seismic interpretation, subsidence analysis and low temperature (U-Th)/He thermochronology. Ph.D. Thesis, Vrije University, Amsterdam, Netherlands, pp. 190.

Mosca, P., Polino, R., Rogledi, S., Rossi, M., 2009. New data for the kinematic interpretation of the Alps–Apennines junction (Northwestern Italy). International Journal of Earth Sciences, DOI 10.1007/s00531-009-0428-2

Negri, A., Giunta, S., Hilgen, F., Krijgsman, W., Vai, G.B., 1999. Calcareous nannofossil biostratigraphy of the Monte del Casino section (Northern Apennines, Italy) and paleoceanographic conditions at the times of late Miocene sapropel formation. Marine Micropaleontology 36, 13-30.

Oliveri, E., Neri, R., Bellanca, A., Riding, R., 2010. Carbonate stromatolites from a Messinian hypersaline setting in the Caltanissetta Basin, Sicily: petrographic evidence of microbial activity and related stable isotope and rare earth element signatures. Sedimentology 57, 142-161.

Orszag-Sperber, F., 2006. Changing perspectives in the concept of Lago-Mare" in Mediterranean Late Miocene evolution. Sedimentary Geology 188–189, 259-277.

Panieri, G., Lugli, S., Manzi, V., Roveri, M., Schreiber, C.B., Palinska, K.A., 2010. Ribosomal RNA gene fragments from fossilized cyanobacteria identified in primary gypsum from the late Miocene, Italy. Geobiology 8, 101-111.

Raffi, I., Mozzato, C., Fornaciari, E., Hilgen, F.J., Rio D., 2003. Late Miocene calcareous nannofossil biostratigraphy and astrochronology for the Mediterranean region. Micropaleontology **49**, 1-26.

Riding, R., Braga, J. C., Martín, J. M., Sánchez-Almazo, I. M., 1998. Mediterranean Messinian Salinity Crisis: constraints from a coeval marginal basin, Sorbas, southeastern Spain. Marine Geology 146, 1-20.

Rossi, M., Mosca, P., Polino, R., Biffi, U., 2009. New outcrop and subsurface data in the Tertiary Piedmont Basin (NW Italy): unconformity bounded stratigraphic units and their relationships with basin modification phases. Rivista Italiana di Paleontologia e Stratigrafia 115, 305-335.

Rouchy, J. M., Caruso, A., 2006. The Messinian Salinity Crisis in the Mediterranean basin: a reassessment of data and an integrated scenario. Sedimentary Geology 188-189, 35-67.

Roure, F., Bergerat, F., Damotte, B., Mugnier, J. L., Polino, R., 1996. The ECORS-CROP Alpine seismic traverse. Bulletin de la Société. Géologique de France 170, 1-113.

Roveri, M., Bassetti, M. A., Ricci Lucchi, F., 2001. The Mediterranean Messinian salinity crisis: an Apennine foredeep perspective. Sedimentary Geology 140, 201-214.

Roveri, M., Manzi, V., Ricci Lucchi, F., Rogledi, S., 2003. Sedimentary and tectonic evolution of the Vena del Gesso basin (Northern Apennines, Italy): implications for the onset of the Messinian salinity crisis. Geological Society of America Bulletin 115, 387-405.

Roveri, M., Manzi, V., 2007. Gessoso-Solfifera, In: Cita, M.B., Abbate, E., Balini, M., Conti, M.A., Falorni, P., Germani, D., Groppelli, G., Manetti, P., Petti, F. M., (Eds), Carta Geologica d'Italia 1:50000, Catalogo delle Formazioni, Unità tradizionali (2). Quaderni Servizio Geologico d'Italia, serie III 7, pp. 303-310.

Roveri, M., Lugli, S., Manzi, V., Schreiber, B.C., 2008a. The Messinian Sicilian stratigraphy revisited: new insights for the Messinian Salinity Crisis. Terra Nova 20, 483-488.

Roveri, M., Lugli, S., Manzi, V., Schreiber, B.C., 2008b. The Messinian Salinity Crisis: a sequence-stratigraphy approach. GeoActa, Special Publication 1, 117-138.

Ryan, W.B.F., 1976. Quantitative evaluation of the depth of the western Mediterranean before, during and after the late Miocene salinity crisis. Sedimentology 23, 791-813.

Ryan, W.B.F., 2009. Decoding the Messinian salinity crisis. Sedimentology 56, 95-136.

Sage, F., von Gronefeld, G., Déverchère, J., Gaullier, V., Gorini, C., 2005. A record of the Messinian salinity crisis on the western Sardinia margin, northwestern Mediterranean. Marine and Petroleum Geology 22, 757-773.

Sardella, R., 2008. Remarks on the Messinian carnivores (Mammalia) of Italy. Bollettino della Società Paleontologica Italiana 47, 195-202.

Schreiber, B.C., 1978. Environments of subaqueous gypsum deposition, In: Dean, W.E., Schreiber, B.C., (Eds.), Marine evaporites. SEPM Shourt Course 4, Oklahoma City, pp. 43-73.

Schreiber, B.C., El Tabakh, M., 2000. Deposition and early alteration of evaporites. Sedimentology 47, 215-238.

Sierro, F.J., Hilgen, F.J., Krijgsman, W., Flores, J.A., 2001. The Abad composite (SE Spain): a Messinian reference section for the Mediterranean and the APTS. Palaeogeography, Palaeoclimatology, Palaeoecology 168, 141-169.

Sturani, C., 1973. A fossil eel (*Anguilla* sp.) from the Messinian of Alba (Tertiary Piedmont Basin). Palaeoenvironmental and palaeogeographic implications, In: Messinian events in the Mediterranean. K. Nederl. Akad. Wetensch., Amsterdam, 243-255.

Sturani, C., 1976. Messinian facies in the Piedmont basin. Memorie della Società Geologica Italiana 16, 11-25.

Sturani, C., Sampò, M., 1973. Il Messiniano inferiore in facies diatomitica nel Bacino Terziario Piemontese. Memorie della Società Geologica Italiana 12, 335-338.

Suc, J.-P., Violanti, D., Londeix, L., Poumot, C., Robert, C., Clauzon, G., Gautier, F., Turon, J.-L., Ferrier, J., Chikhi, H., Cambon, G., 1995. Evolution of the Messinian Mediterranean environments: the Tripoli Formation at Capodarso (Sicily, Italy). Review of Palaeobotany and Palynology 87, 51-79.

Vai, G.B., 1997, Cyclostratigraphic estimate of the Messinian stage duration, In: Montanari, A., Odin, G.S., Coccioni, R., (Eds.), Miocene stratigraphy—An integrated approach. Elsevier, Amsterdam, pp. 463-476.

Vai, G.B., Ricci Lucchi, F., 1977. Algal crusts, autochtonous and clastic gypsum in a cannibalistic evaporite basin; a case history from the Messinian of Northern Apennine. Sedimentology 24, 211-244.

van Morkhoven, F.P.C.M., Berggren, W.A., Edwards, A.S., 1986. Cenozoic cosmopolitan deep-water benthic foraminifera. Bulletin Centres Recherches Exploration-Production Elf-Aquitaine, Memories 11, pp. 421.

Vasconcelos, C., McKenzie, J.A., Bernasconi, S., Grujic, D., Tien, A.J., 1995. Microbial mediation as a possible mechanism for natural dolomite formation at low temperatures. Nature **377**, 220-222.

Vazquez, A., Utrilla, R., Zamarreno, I., Sierro, F.J., Flores, J.A., Francés, G., Bàrcena M.A., 2000. Precession-related sapropelites of the Messinian Sorbas Basin (South Spain): paleoenvironmental significance. Palaeogeography, Palaeoclimatology, Palaeoecology 158, 353-370.

Violanti, D., Gallo, L.M., Rizzi, A., 2007. Foraminiferal assemblages of the Bric della Muda laminites (Nizza Monferrato, Piedmont): proxies of cyclic paleoenvironmental changes in the lower Messinian of North-Western Italy. Geobios 40, 281-290.

Violanti, D., Trenkwalder, S., Lozar, F., Gallo, L.M., 2009. Micropalaeontological analyses of the Narzole core: biostratigraphy and palaeoenvironment of the late Messinian and early Zanclean of Piedmont (Northwestern Italy). Bollettino della Società Paleontologica Italiana 48, 167-181.

Wade, B.S., Bown, P., 2006. Calcareous nannofossils in extreme environments: the Messinian Salinity Crisis, Polemi Basin, Cyprus. Palaeogeography, Palaeoclimatology, Palaeoecology 233, 271-286.

Wright, R., 1978. Neogene paleobathymetry of the Mediterranean based on benthic foraminifers from DSDP Leg 42A, In: Kidd, R.B., Worstell, P.J., (Eds.), Initial Report of the Deep Sea Drilling Project 42. U.S. Government Printing Office, Washington DC, pp. 837-846.

Wright, D.T., Oren, A., 2005. Nonphotosynthetic bacteria and the formation of carbonates and evaporites through time. Geomicrobiology Journal **22**, 27-53.

Figure captions

Fig. 1. Geologic and structural map of northwestern Italy and location of the studied area (modified from Bigi et al., 1990). TH: Torino Hill; MO: Monferrato, AM: Alto Monferrato; BG: Borbera Grue; SVZ: Sestri Voltaggio fault zone; VVL: Villalvernia–Varzi line. IL: Insubric line; TPB: Tertiary Piedmont Basin.

Fig. 2. Schematic geologic map of the studied area and location of the stratigraphic sections. A) Arnulfi; B) Rio Berri; C) Cascina Merlotti; D) Rocca del Campione; E) Pollenzo; F) Santa Vittoria d'Alba.

Fig. 3. A) Regional profile across the Savigliano basin and adjacent regions in a N-S direction (redrawn after Bertotti and Mosca, 2009 and Mosca et al., 2009). The trace of the profile is reported in Fig. 1. B) Schematic cross section, flattened at the base of the Pliocene, showing the relationships between the Messinian units. Not to scale. PLG: Primary Lower Gypsum; RLG: Resedimented Lower Gypsum; CRB: carbonate-rich beds; SKB: Sturani key-bed; MES: Messinian erosional surface.

Fig. 4. The composite Messinian section of Alba reconstructed by Sturani (1973). TO: upper Tortonian silty clays and marls; 1: lower Messinian silts and clays; 2: thinly laminated silty clays with beds of stromatolitic limestone; 3a: sulphate-rich euxinic clays with lenses of early diagenetic selenite; 3b: laminated microcrystalline primary gypsum bed; 4a: laminated silts and silty marls; 4b) thick bed of selenite crystals conglomerates; 5: current-laminated fine sands and massive clays; PL: normal marine Pliocene silty clays and marls. A: planktonic foraminifers; B: benthic foraminifers; C: spatangoid echinoids; D: lantern fish (*Myctophum* sp.); E: *Galeoidea echinophora*; F: ahermatypic corals; G: pteropods (*Cavolinia gypsorum*); H: planktonic diatoms; I: *Rectuvigerina*

tenuistriata; J: land floras; K: cyprinodont fish (*Pachylebias* sp., now *Aphanius* sp.); L: *Spratelloides* sp.; M: dragonfly larva; N: young eel (*Anguilla* sp.); O: small sole (*Microchirus bassanianus*); P: adult dragonfly; Q; land turtle (*Testudo craverii*); R: freshwater reeds (*Phragmites oeningensis*); S*: in situ* roots; T: *Pycnodonta cochlear.*

Fig. 5. The Arnulfi section (left) and detail of the transition between the Sant'Agata Fossili Marls and the Primary Lower Gypsum (right). The lithologic cycles discussed in the text (Am1-Am5; Ag1-Ag6) are shown. The abundance and distribution of selected calcareous nannofossil and foraminifer taxa are also reported. The benthic foraminifer assemblages are described in the text. SKB: Sturani key-bed; CSC: Cassano Spinola Conglomerates.

Fig. 6. The Pollenzo section (left) and detail of the upper part of the Sant'Agata Fossili Marls and of the Primary Lower Gypsum unit (right). The lithologic cycles discussed in the text are reported. Letters in italics (*a* to *g*) indicate the carbonate-rich beds. The carbonate content of the upper part of Sant'Agata Fossili Marls is also indicated. SKB: Sturani key-bed; RLG: Resedimented Lower Gypsum (VVC: Valle Versa chaotic complex); AAF: Argille Azzurre Fm. Micropaleontological data are from Lozar et al. (2010).

Fig. 7. Panoramic view of the lower part of the Pollenzo section, showing the boundary between the Sant'Agata Fossili Marls (SAF) and the Primary Lower Gypsum unit (PLG). The letters indicate the carbonate-rich beds discussed in the text, that are recognizable for their whitish colour. Carbonate-rich beds belonging to cycles Pm1 and Pm2 (*a* and *b*) are not visible.

Fig. 8. Pollenzo section**.** A) Outcrop view of cycles Pm3, Pm4 and Pm5. The carbonate- rich beds *c*, *d* and *e* are visible. B) Photomicrograph of the 6th bed (*f*): a network of empty fissures, oriented both parallel and perpendicular to bedding, is recognizable. C) SEM image of a slightly etched broken chip of the first bed (*a)* showing euhedral dolomite crystals. D) SEM image of a slightly etched broken chip of the 7th bed (*g)*: a rounded dolomite crystal with a central hollow is recognizable (white arrow). The EDS analysis of the crystal is shown. E) SEM image of a pyrite framboid in the 5th bed (*e*).

Fig. 9. Arnulfi section. A) Panoramic view of the upper part of the Arnulfi section. The fourth (Ag4) and fifth (Ag5) gypsum beds are visible under the trees. The sixth gypsum bed (Sturani key-bed: SKB) is also recognizable. B) First gypsum bed composed of vertically-oriented twinned massive

selenite. C) Fourth gypsum bed: different layers of vertically-oriented crystals, separated by sharp surfaces, are visible.

Fig. 10. A) The Sturani key-bed at Arnulfi: clustered flat conical features (branching selenite) are recognizable within the laminated matrix (indicated by the black arrow). B) SEM image of a broken chip of a gypsum lamina, showing tiny euhedral crystals randomly distributed on the lamina surface. A twinned crystal is recognizable in the upper right of the image. C) Close up of a cone with horizontally-oriented selenite crystals. The pencil is 3 cm long. D) Polished slab of the Sturani key-bed, cut perpendicularly to the bedding: "nodular" features (branching selenite) composed of centimetre-sized crystals are recognizable within the laminated matrix.

Fig. 11. Pollenzo section. A) Massive selenite bed belonging to cycle Pg2. B) Outcrop view of cycle Pg3 with the Sturani key-bed (SKB) and the underlying mudstone layer (m. The dotted line indicates the boundary between cycle Pg3 and the underlying selenite bed of cycle Pg2. C) Close up of the Sturani key-bed: note the finely laminated structure and the occurrence, in the lower part, of lenticular features composed of coarser gypsum crystals (arrows), corresponding to branching selenite. D) Metre-sized flat conical feature (branching selenite) at the base of the Sturani key-bed, grown within the laminated matrix (lm).

Fig. 12. A) Upper PLG cycles at Pollenzo: four cycles (Pg4-Pg7), made up of mudstones and thin gypsum beds, are recognizable above the Sturani key-bed (SKB). B) Outcrop view of the gypsum bed of cycle Pg4, consisting of flat conical features (arrows) within a laminated matrix (lm). C) Photomicrograph of a gypsum bed belonging to the upper PLG cycles: dissolved gypsum crystals that are partially replaced by calcite, are visible.

Fig. 13. Pollenzo section. A) Strongly deformed muddy sediments and carbonate beds (arrows) belonging to the slumped interval above the PLG unit. Hammer for scale. B) The unconformity separating the slumped interval (SI) below, from fine-grained sediments belonging to the Cassano Spinola Conglomerates (CSC) above.

Fig. 14. Correlation scheme of the studied sections. Datum plane: base of the Sturani key-bed. Symbols are the same as in Figs. 5 and 6. The correlation with the Alba section of Sturani (1973), reported in Fig. 4, is shown. Yellow stripes: carbonate-rich beds; blue lines: discontinuity surfaces. RLG: Resedimented Lower Gypsum; MES: Messinian Erosional Surface.

Fig. 15. Stratigraphic model of the MSC record of Alba. A) cross section flattened at the base of the Pliocene. B) chronostratigraphic scheme. PLG: Primary Lower Gypsum; RLG: Resedimented Lower Gypsum. SKB: Sturani key-bed; MES: Messinian erosional surface. Stratigraphic sections: A) Arnulfi; B) Rio Berri; C) Cascina Merlotti; D) Rocca del Campione; E) Pollenzo; F) Santa Vittoria d'Alba.

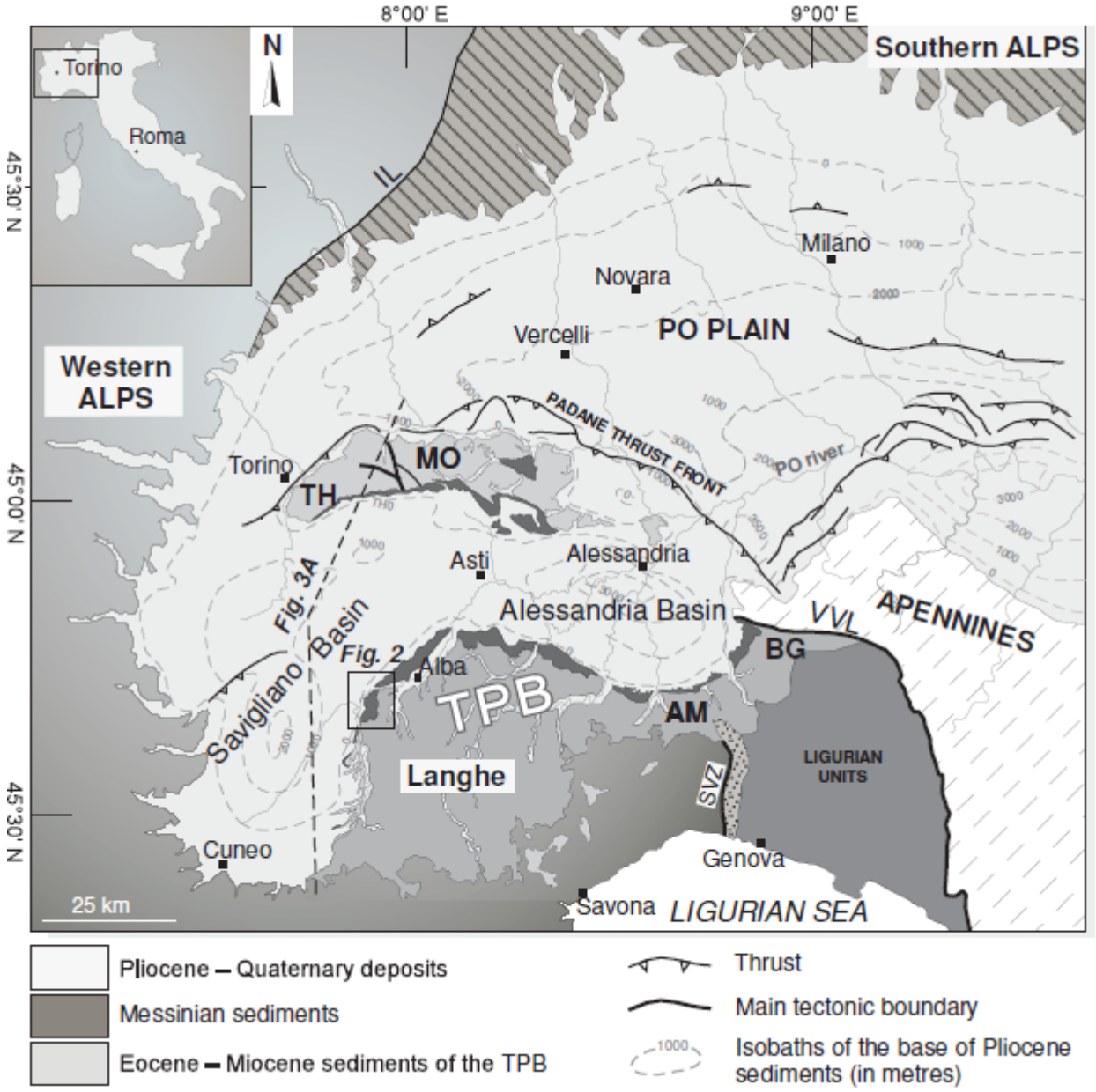

Dela Pierre et al. Fig.1

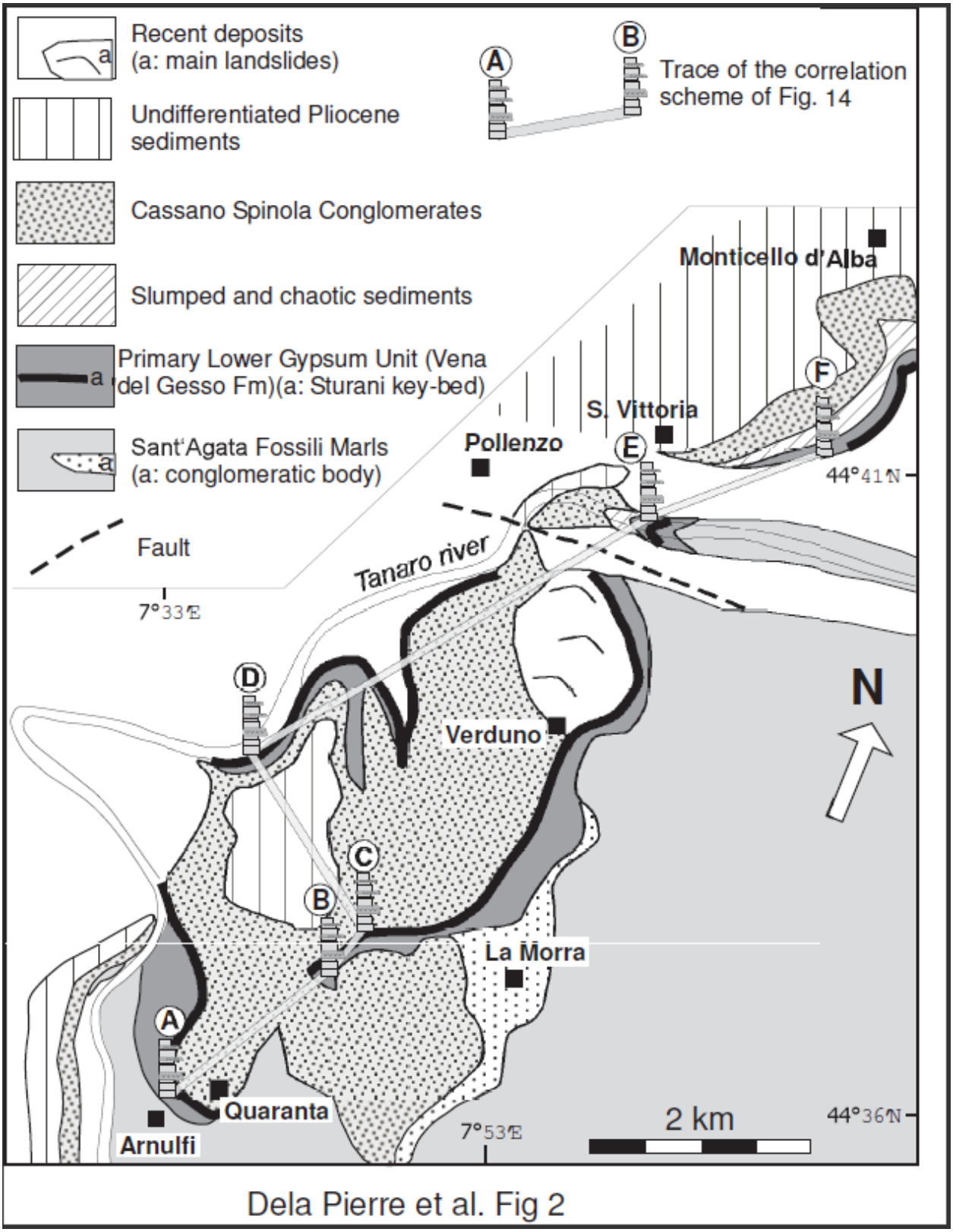

Dela Pierre et al. Fig 2

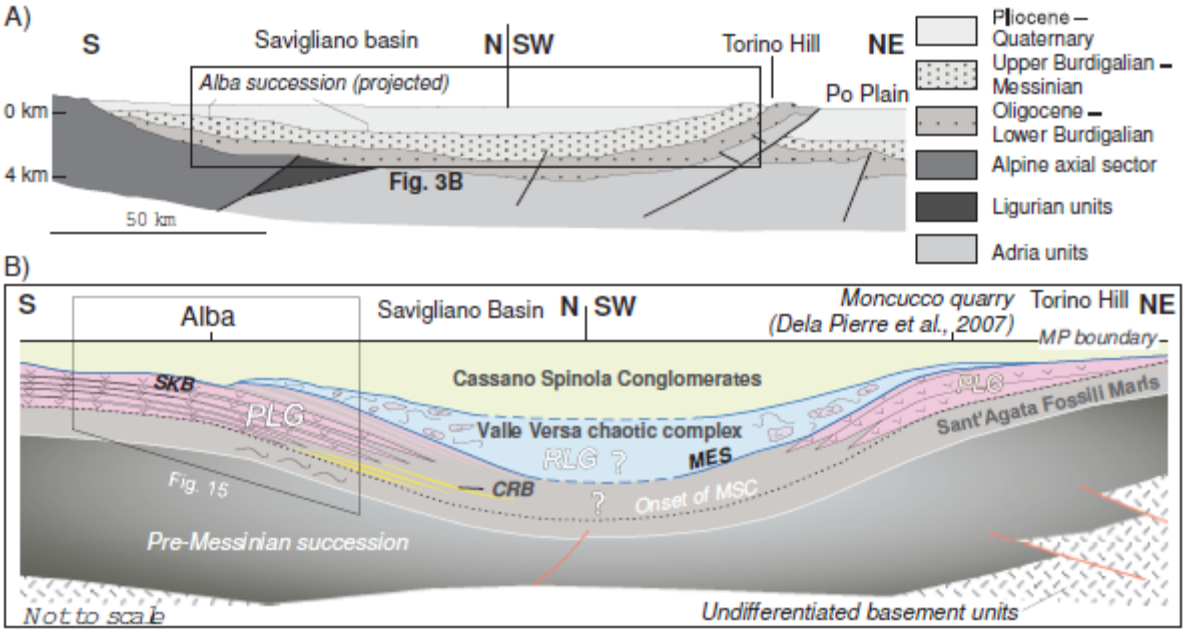

Dela Pierre et al., Fig. 3

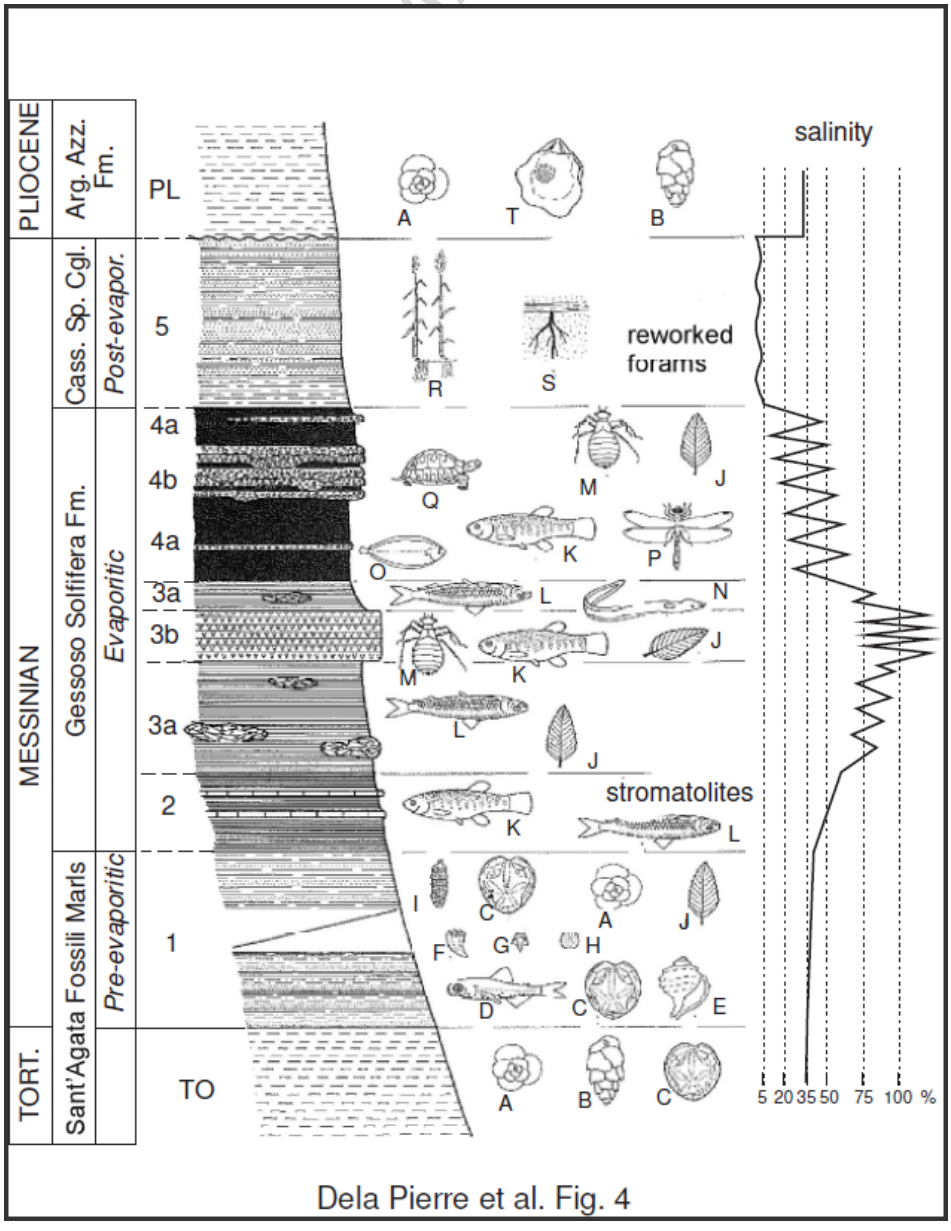

Dela Pierre et al. Fig. 4

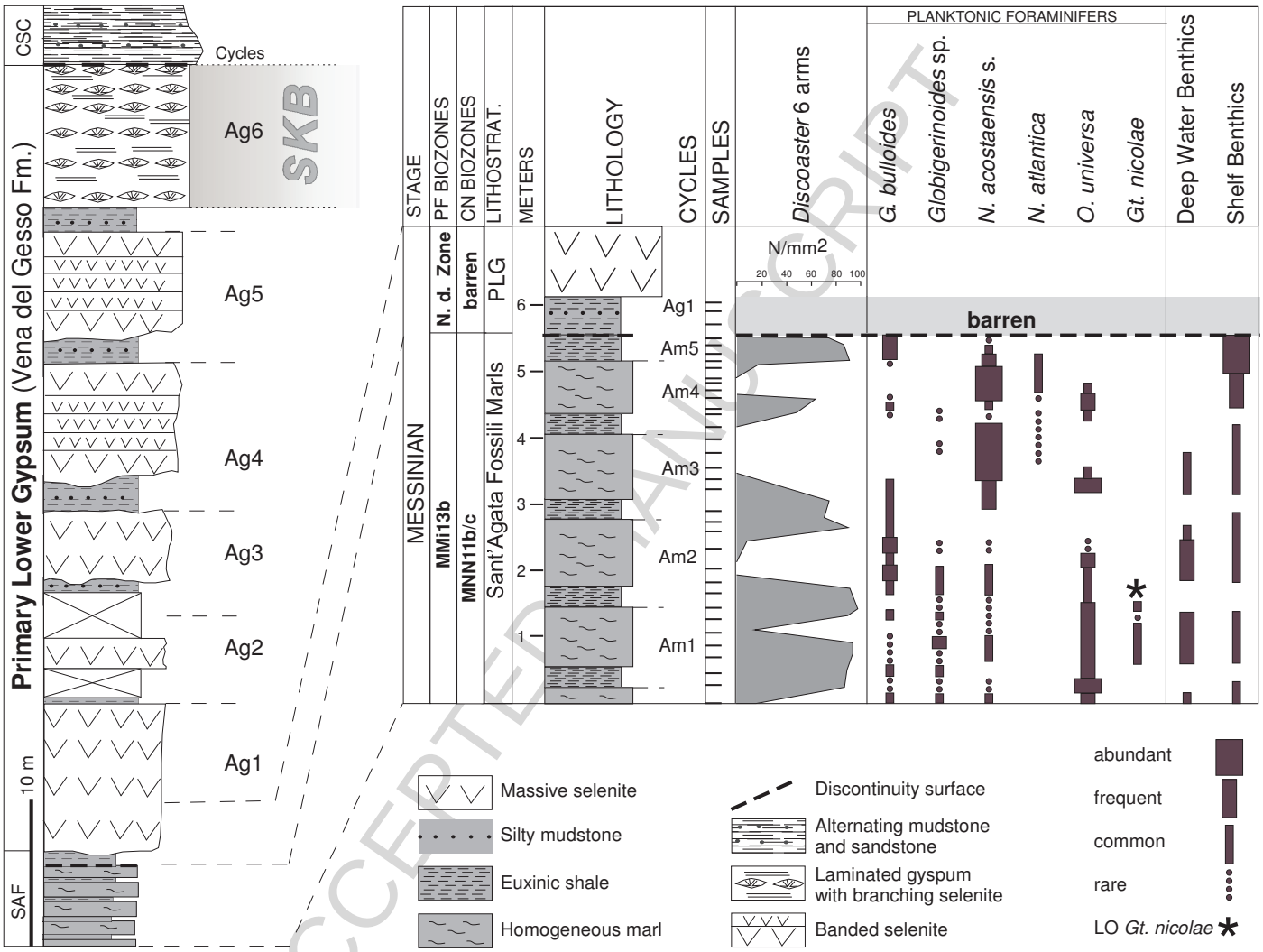

Dela Pierre et al.Fig. 5

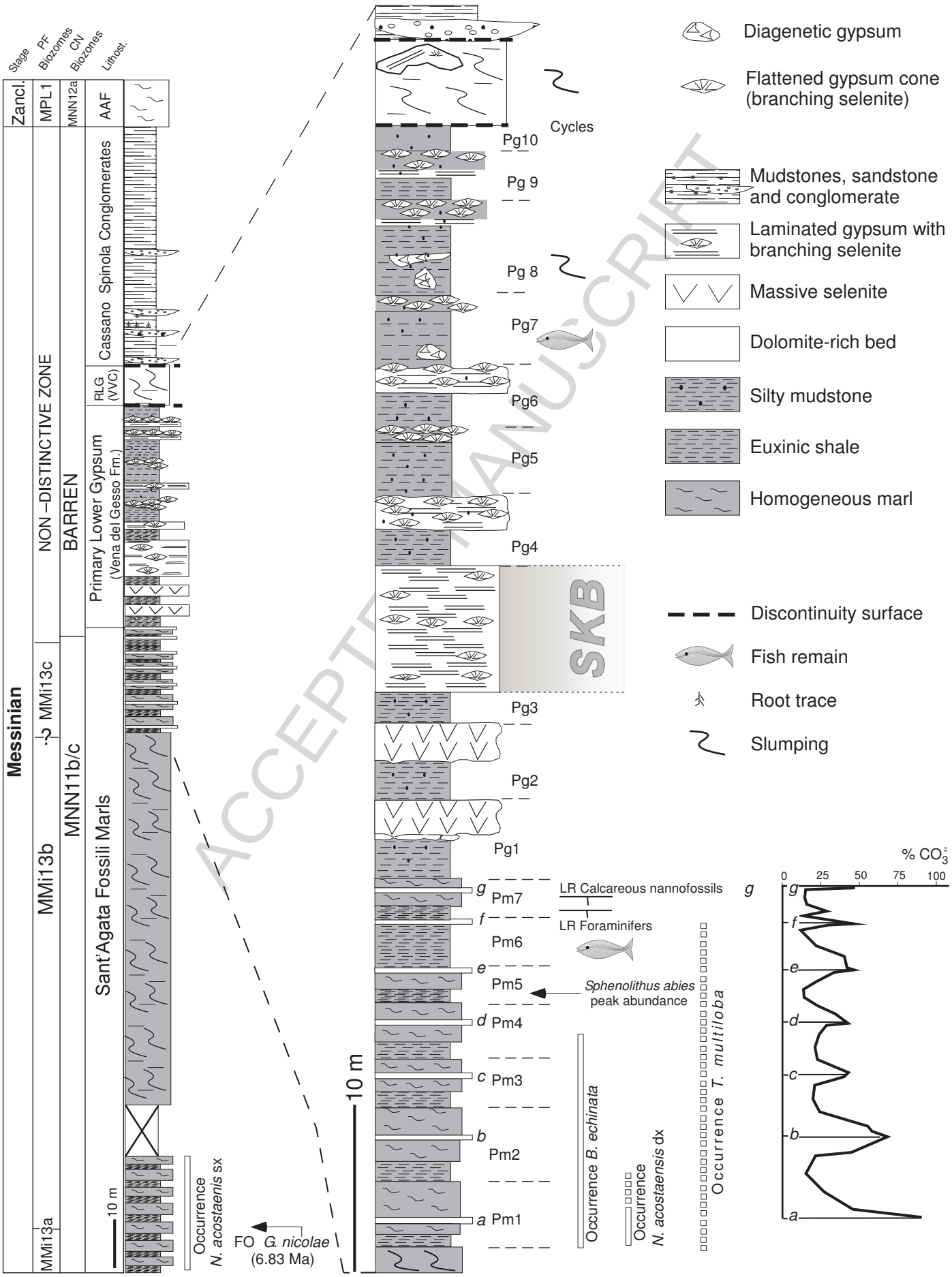

Dela Pierre et al., Fig. 6

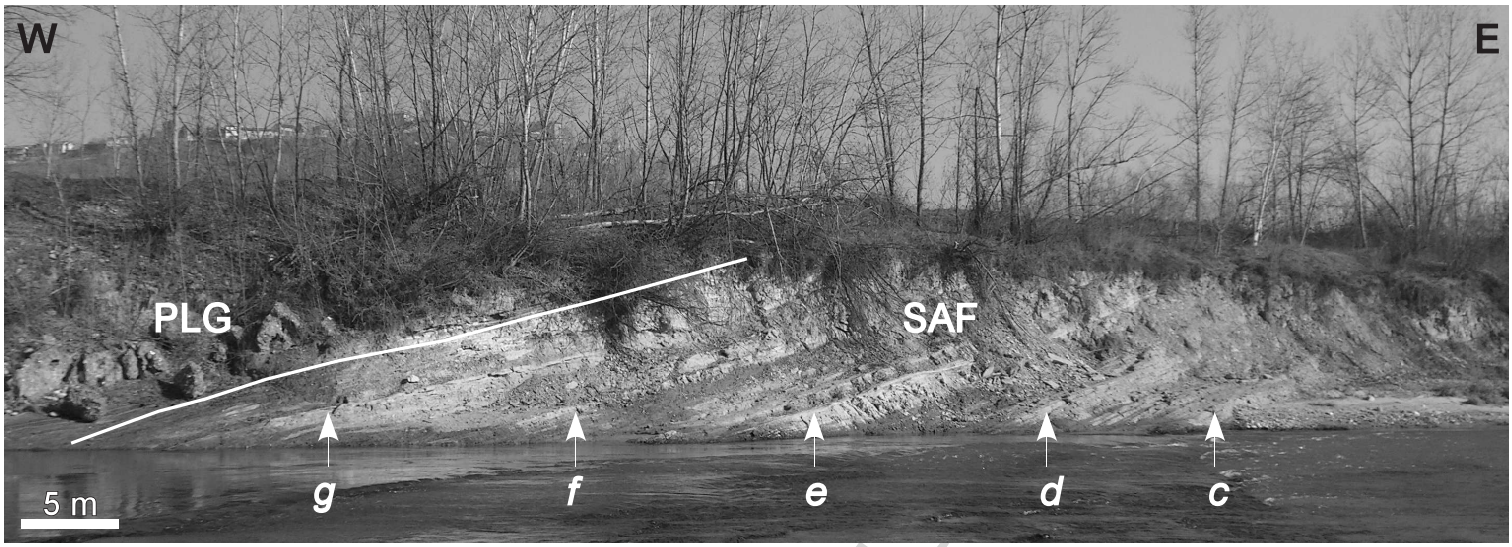

Dela Pierre et al. Fig.7

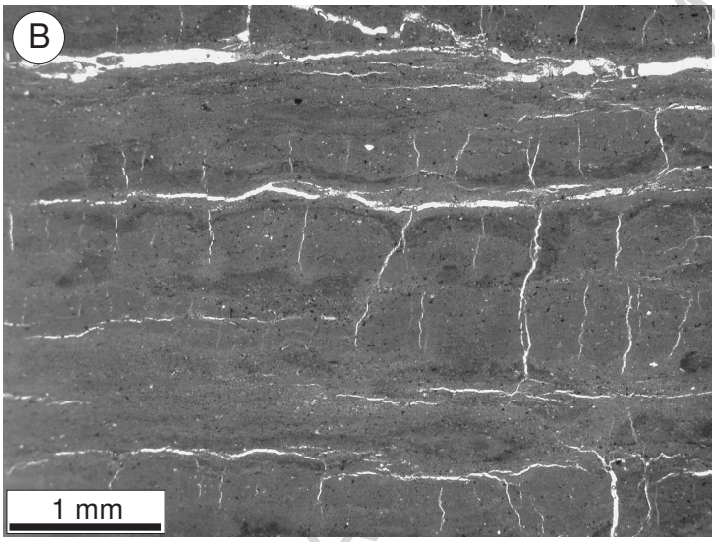

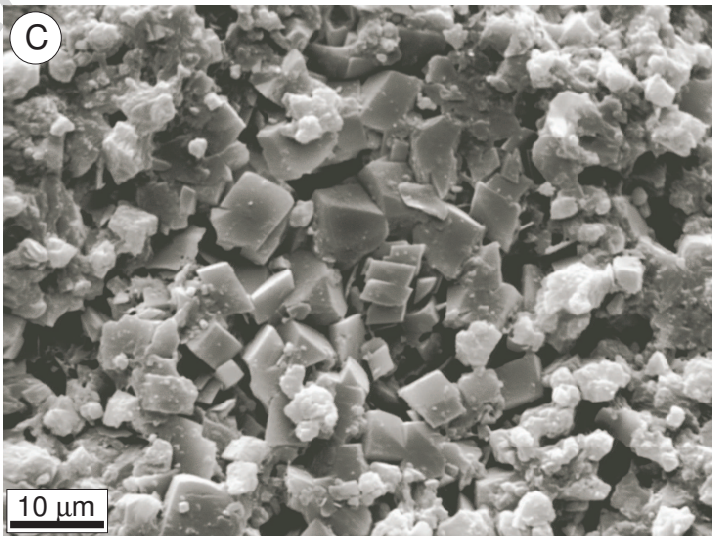

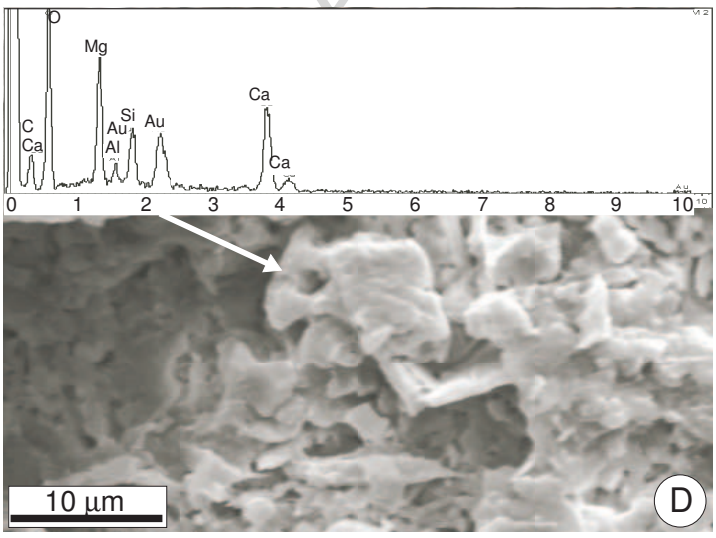

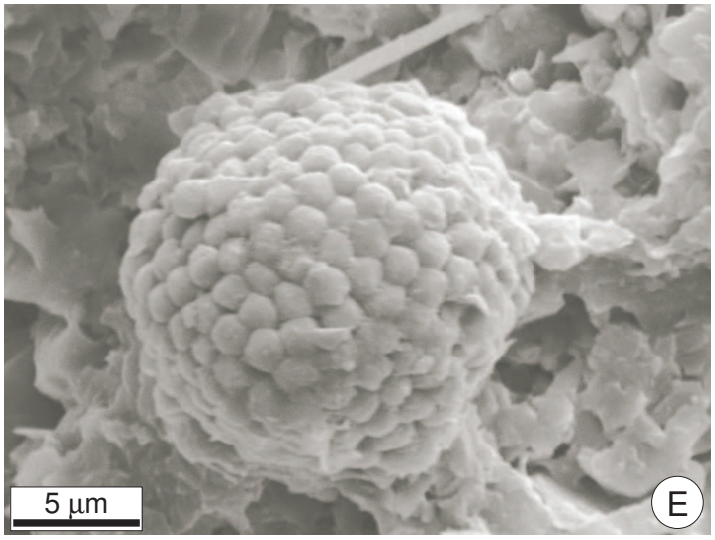

Dela Pierre et al. Fig.8

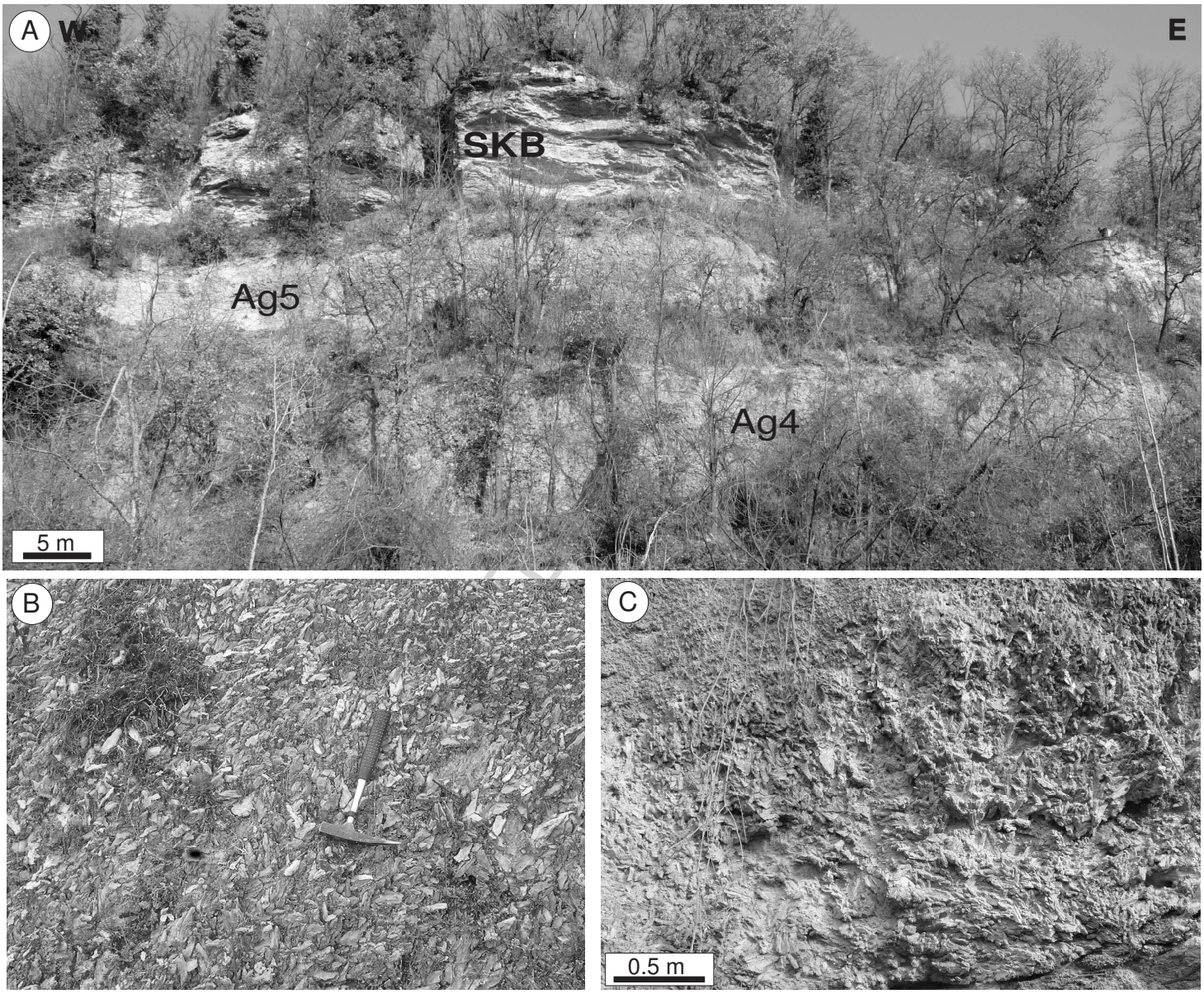

Dela Pierre et al. Fig.9

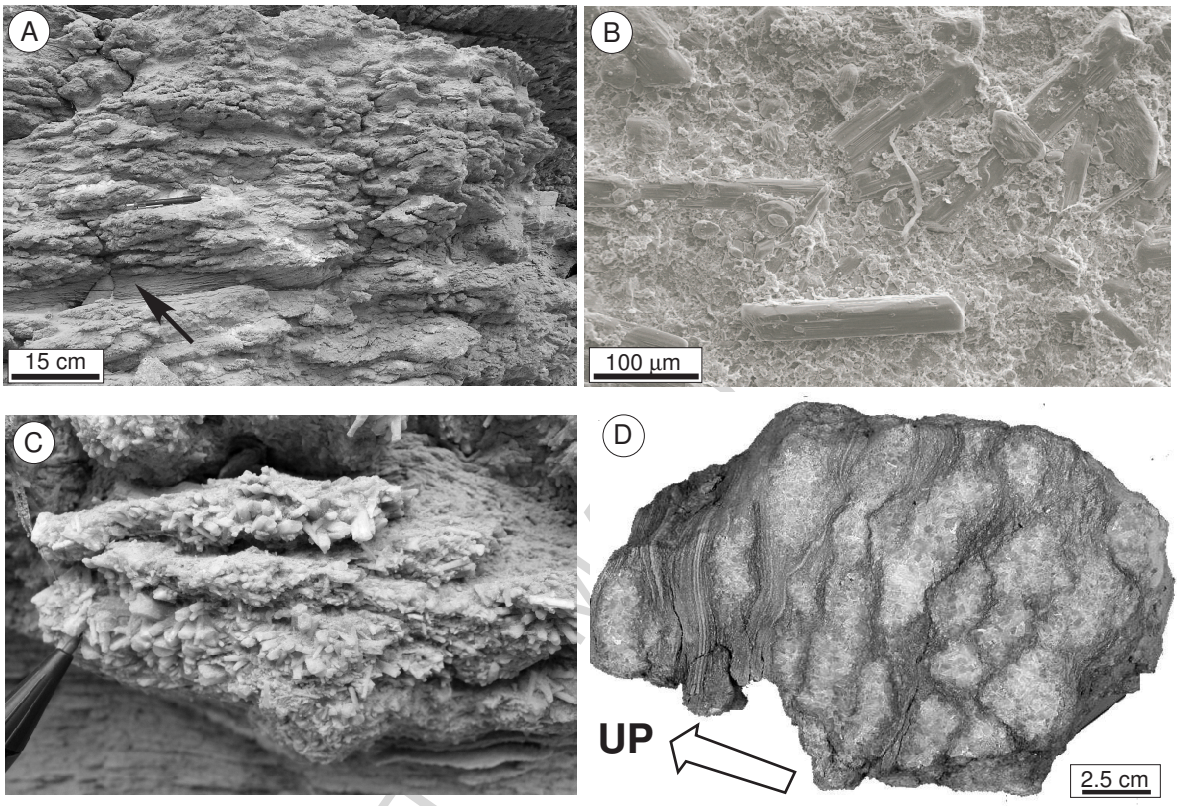

Dela Pierre et al. Fig.10

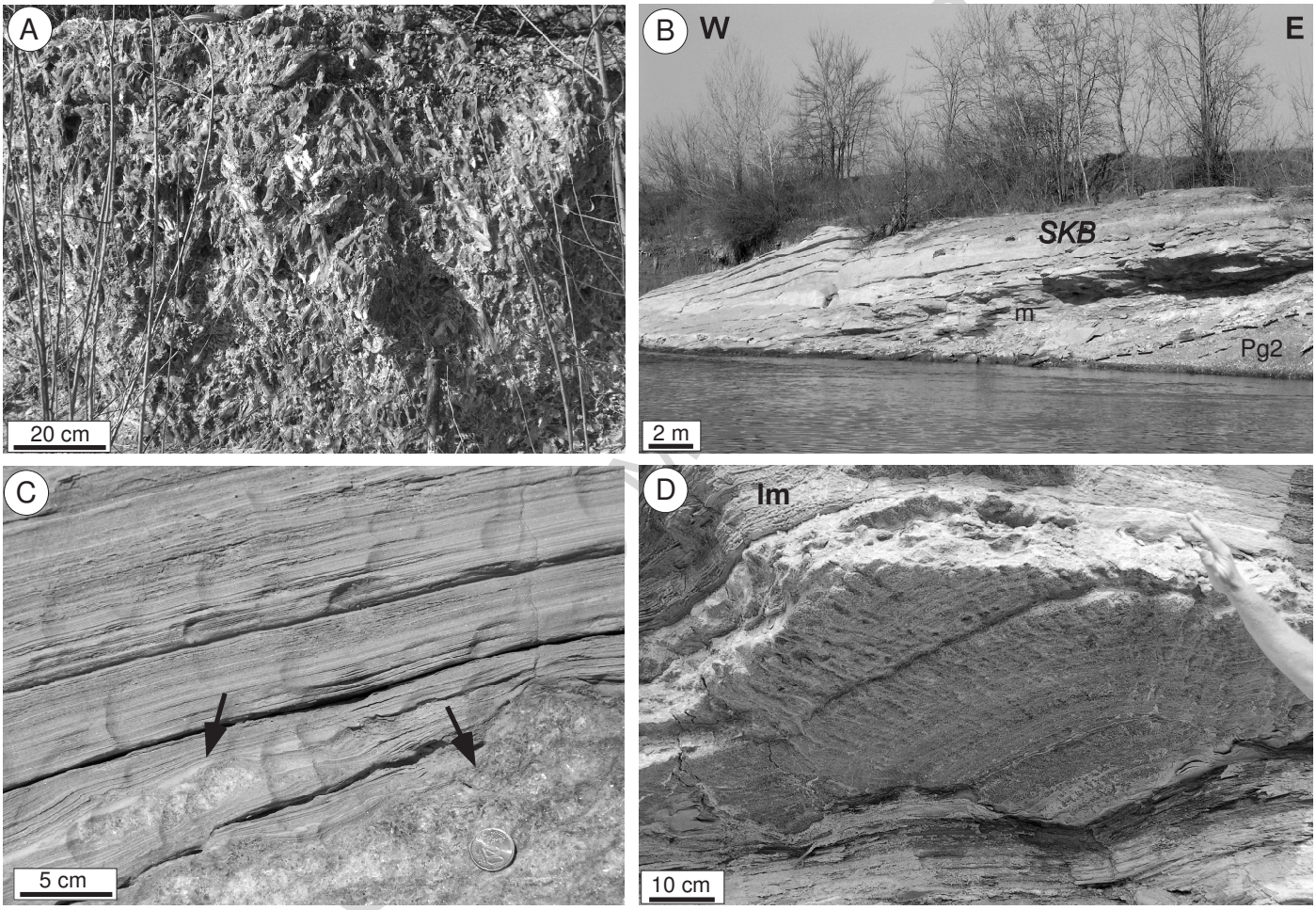

Dela Pierre et al. Fig. 11

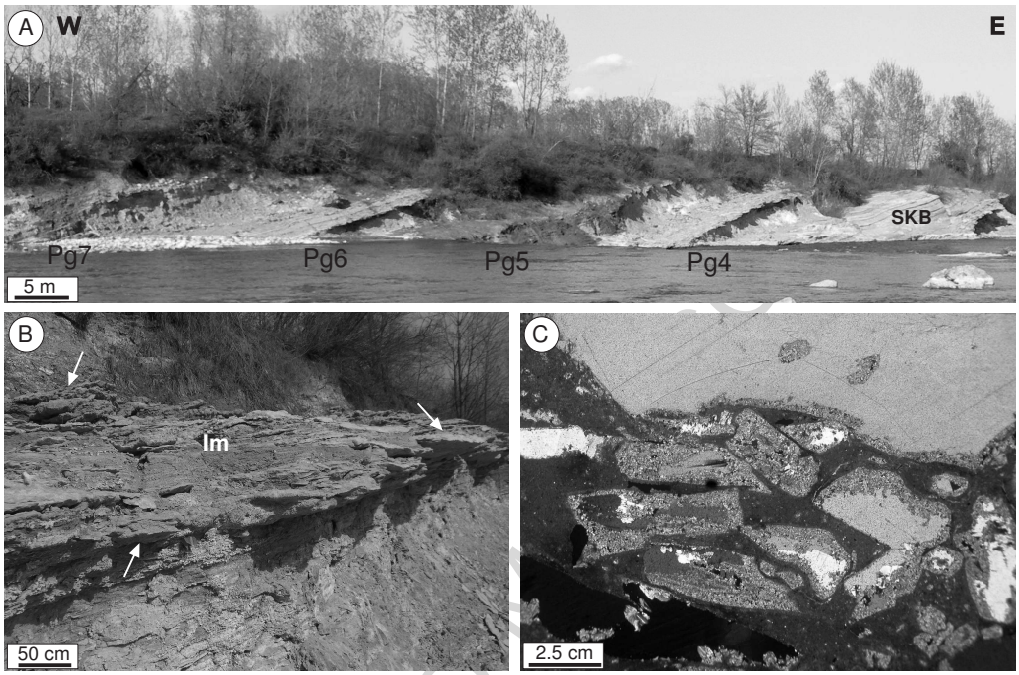

Dela Pierre et al. Fig.12

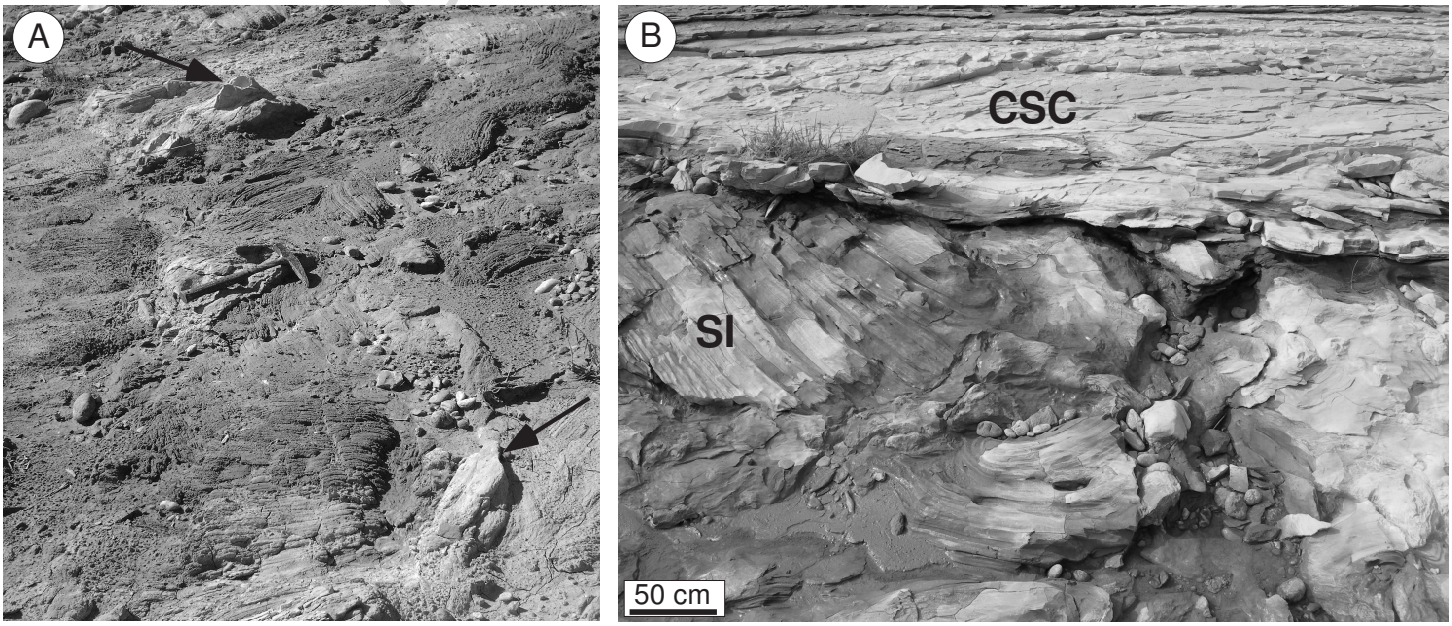

Dela Pierre et al. Fig.13

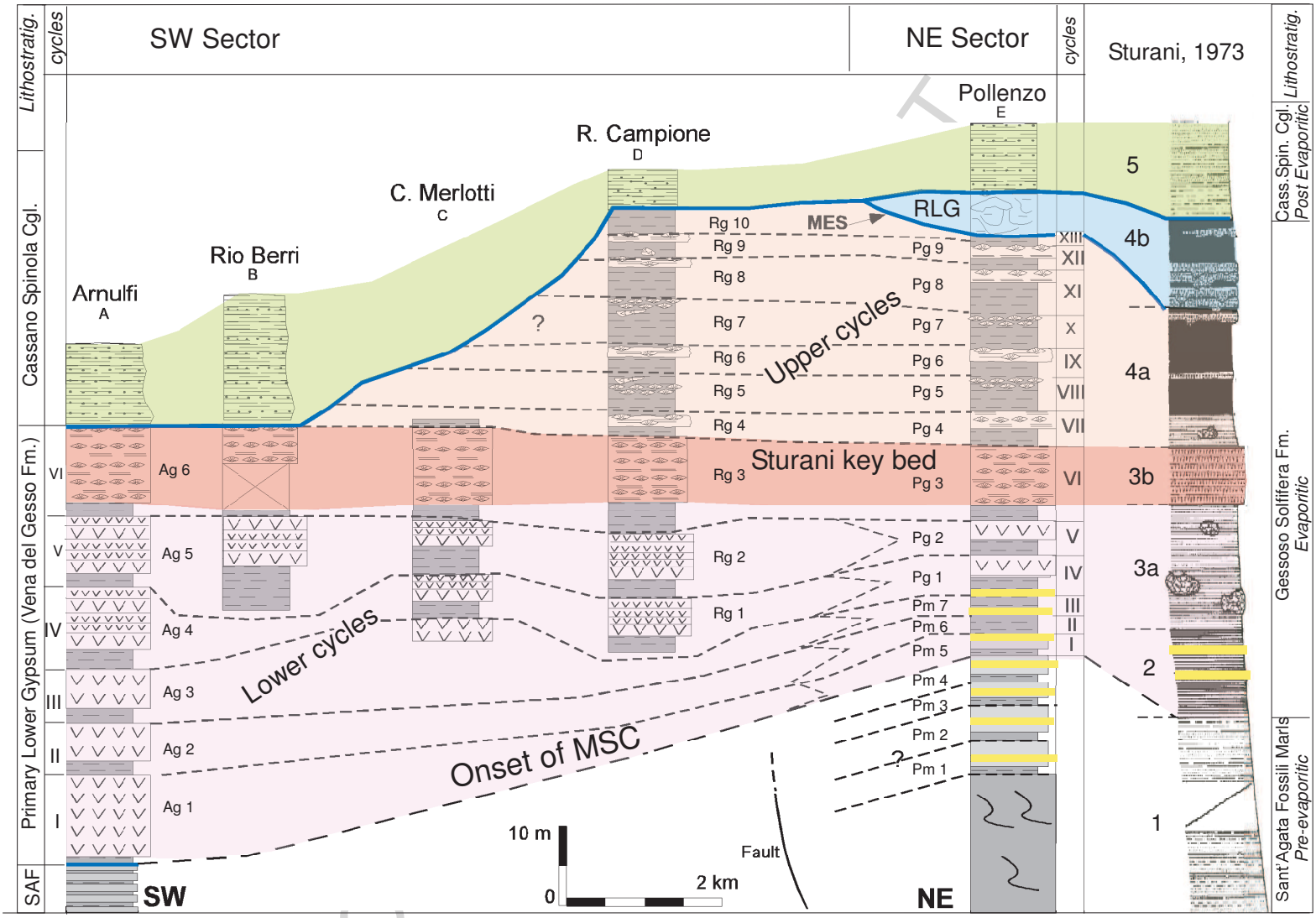

Dela Pierre et al. Fig. 14

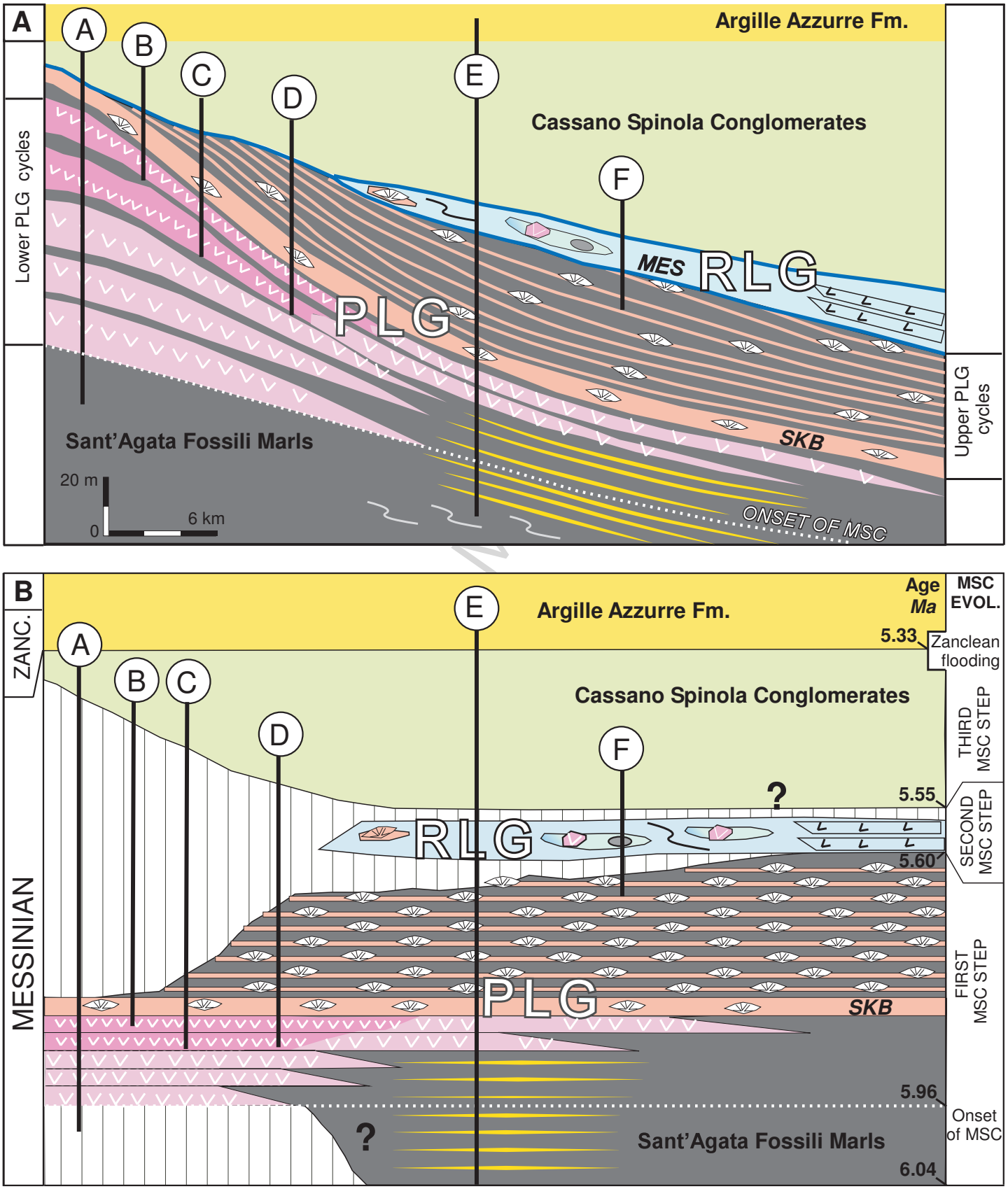

Dela Pierre et al. Fig. 15

Research highlights

- Updated stratigraphy of the northernmost record of the Messinian salinity crisis
- Reconstruction of the lateral transition between marginal and distal settings
- Influence of climate gradients on the sedimentary response to the salinity crisis